

# Summer rainfall dissolved organic carbon, solute, and sediment fluxes in a small Arctic coastal catchment on Herschel Island (Yukon Territory, Canada)

Caroline Coch, Scott F. Lamoureux, Christian Knoblauch, Isabell Eischeid, Michael Fritz, Jaroslav Obu, and Hugues Lantuit

**Abstract:** Coastal ecosystems in the Arctic are affected by climate change. As summer rainfall frequency and intensity are projected to increase in the future, more organic matter, nutrients and sediment could be mobilized and transported into the coastal nearshore zones. However, knowledge of current processes and future changes is limited. We investigated streamflow dynamics and the impacts of summer rainfall on lateral fluxes in a small coastal catchment on Herschel Island in the western Canadian Arctic. For the summer monitoring periods of 2014–2016, mean dissolved organic matter flux over 17 days amounted to  $82.7 \pm 30.7 \text{ kg km}^{-2}$  and mean total dissolved solids flux to  $5252 \pm 1224 \text{ kg km}^{-2}$ . Flux of suspended sediment was  $7245 \text{ kg km}^{-2}$  in 2015, and  $369 \text{ kg km}^{-2}$  in 2016. We found that 2.0% of suspended sediment was composed of particulate organic carbon. Data and hysteresis analysis suggest a limited supply of sediments; their interannual variability is most likely caused by short-lived localized disturbances. In contrast, our results imply that dissolved organic carbon is widely available throughout the catchment and exhibits positive linear relationship with runoff. We hypothesize that increased projected rainfall in the future will result in a similar increase of dissolved organic carbon fluxes.

*Key words:* permafrost, hydrology, lateral fluxes, hysteresis, climate change.

**Résumé :** Les écosystèmes côtiers dans l'Arctique sont touchés par le changement climatique. Comme la fréquence et l'intensité des pluies d'été sont censées augmenter à l'avenir, plus de matière organique, de substances nutritives et de sédiments pourraient être mobilisés et transportés dans les zones proches des côtes. Par contre, la connaissance quant aux processus actuels et quant aux changements futurs est limitée. Nous avons examiné la dynamique de débit d'eau et les impacts des pluies d'été sur les flux latéraux dans un petit

Received 3 May 2018. Accepted 5 July 2018.

**C. Coch and H. Lantuit.** Department of Periglacial Research, Helmholtz Centre for Polar and Marine Research, Alfred Wegener Institute, Telegrafenberg A45, Potsdam 14473, Germany; Institute of Earth and Environmental Science, University of Potsdam, Karl-Liebknecht-Straße 24/25, Potsdam 14476, Germany.

**S.F. Lamoureux.** Department of Geography and Planning, Queen's University, Mackintosh-Corry Hall, Room E208, Kingston, ON K7L 3N6, Canada.

**C. Knoblauch.** Institute of Soil Science, Universität Hamburg, Allende-Platz 2, Hamburg 20146, Germany.

**I. Eischeid.** Norwegian Polar Institute, Framsenteret, Hjalmar Johansens gate 14, Tromsø 9296, Norway.

**M. Fritz.** Department of Periglacial Research, Helmholtz Centre for Polar and Marine Research, Alfred Wegener Institute, Telegrafenberg A45, Potsdam 14473, Germany.

**J. Obu.** Section of Physical Geography and Hydrology, Geologibygningen, University of Oslo, Sem Sælands vei 1, Oslo 0371, Norway.

**Corresponding author:** Caroline Coch (e-mail: [caroline.coch@awi.de](mailto:caroline.coch@awi.de)).

Mark L. Mallory currently serves as an Associate Editor; peer review and editorial decisions regarding this manuscript were handled by Greg Henry.

This article is open access. This work is licensed under a Creative Commons Attribution 4.0 International License (CC BY 4.0). [http://creativecommons.org/licenses/by/4.0/deed.en\\_GB](http://creativecommons.org/licenses/by/4.0/deed.en_GB).

bassin hydrologique côtier de l'île Herschel dans l'ouest de l'Arctique canadien. Pour les périodes de surveillance d'été de 2014–2016, le flux moyen de matière organique dissoute au cours de 17 jours s'est chiffré à  $82,7 \pm 30,7 \text{ kg km}^{-2}$  et le flux moyen du total de matière solide dissoute, à  $5252 \pm 1224 \text{ kg km}^{-2}$ . Le flux de sédiments en suspension était de  $7245 \text{ kg km}^{-2}$  en 2015, et de  $369 \text{ kg km}^{-2}$  en 2016. Nous avons constaté que 2,0 % de la composition de sédiments en suspension constituait du carbone organique en particules. L'analyse des données et de l'hystérèse suggèrent un volume limité de sédiments; leur variabilité interannuelle est très probablement causée par des perturbations localisées de courte durée. Au contraire, nos résultats laissent penser que la matière organique dissoute est largement disponible partout dans le bassin hydrologique et montre une relation linéaire positive avec l'écoulement. Nous formulons l'hypothèse qu'à l'avenir les pluies accrues prévues entraîneront une augmentation semblable du flux de matière organique dissoute. [Traduit par la Rédaction]

*Mots-clés* : pergélisol, hydrologie, flux latéraux, hystérèse, changement climatique.

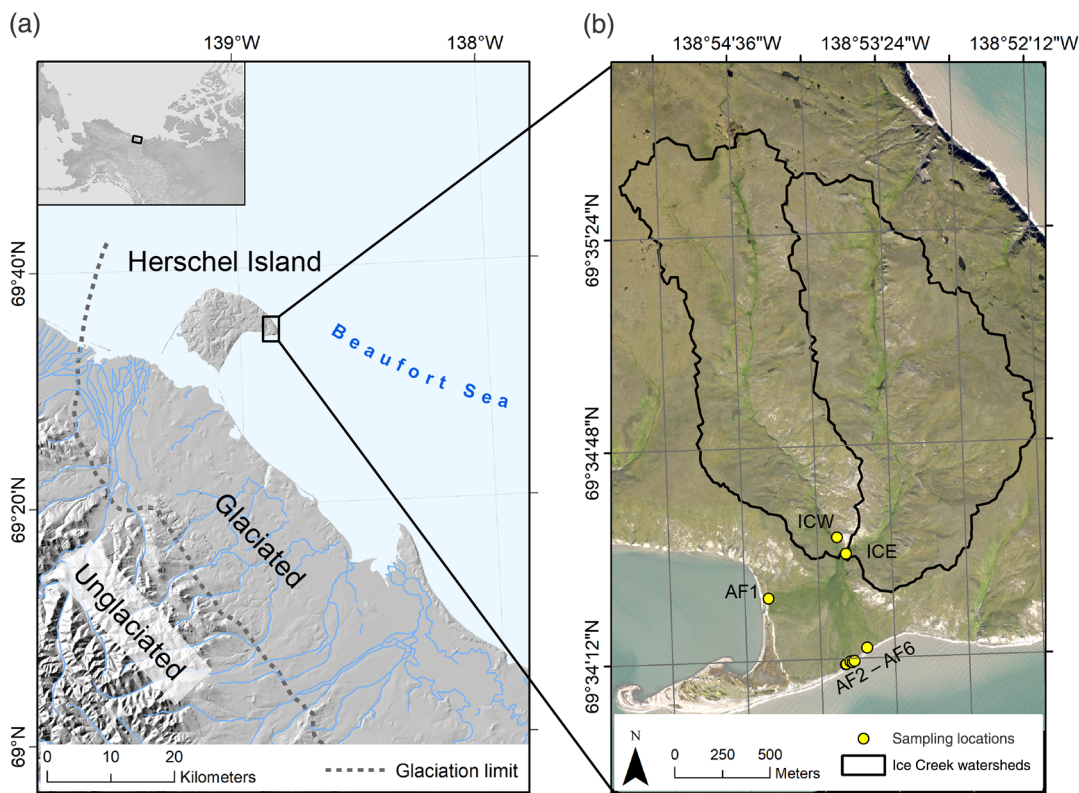
## Introduction

Climate change has important impacts on terrestrial and marine Arctic ecosystems. As rainfall frequency and intensity are projected to increase in the future (Bintanja and Andry 2017), more organic matter, nutrients, and sediment could be mobilized and transported from coastal areas into nearshore zones of the Arctic Ocean. The eight largest Arctic Rivers cover 53% of the Arctic drainage basin, and contribute major fluxes of water and material to the Arctic Ocean (Holmes et al. 2002, 2012; Peterson et al. 2002; Gordeev 2006; Wegner et al. 2015). The remaining 47% of the Arctic drainage basin is characterized by smaller watersheds, where very limited flux estimates are available.

Lateral transport of dissolved organic carbon (DOC), total dissolved solids (TDS), and suspended sediment (SS) is strongly influenced by permafrost coverage, ground ice, topography, soil and vegetation types, and varies across the Arctic region (Vonk et al. 2015; Tank et al. 2018). To investigate sources and flow pathways of a catchment, the dynamic relationship between discharge and hydrochemical concentration for separate hydrographs is studied over time. Hysteresis refers to the cyclical pattern that forms when concentrations at a given discharge differ on the rising and falling limb of the hydrograph. Clockwise hysteresis loops are generally interpreted to indicate a limitation or a source close to the channel outflow. Anti-clockwise or counter-clockwise loops imply a source further away from the outlet, or a late availability of material (Klein 1984). Only few studies examine hysteresis patterns and fluxes of DOC, TDS, and sediment as summarized here.

DOC is positively correlated with discharge in subarctic locations. The hysteresis pattern there varies between studies showing a clockwise behaviour (Carey 2003; Spence et al. 2015) or an anti-clockwise relationship (Petrone et al. 2007). Rain events lead to a dilution of base-flow water and thus, to a decline of major ion concentrations (MacLean et al. 1999; Petrone et al. 2007). Hysteresis patterns for calcium and potassium are clockwise across catchments with varying permafrost coverage (Petrone et al. 2007). The majority of SS is transported during the snowmelt season (Braun et al. 2000; Forbes and Lamoureux 2005; Cockburn and Lamoureux 2008; Lamb and Toniolo 2016; Lamoureux and Lafrenière 2017), although high amounts of sediment may also be mobilized during summer rainfall events (Lewis et al. 2005; Dugan et al. 2012; Lamb and Toniolo 2016). Clockwise suspended sediment discharge hysteresis behaviour suggests a limitation and therefore rapid exhaustion of sediment that can be mobilized during rainfall (Dugan et al. 2009). As specific suspended sediment yield is known to increase with decreasing watershed size (Walling 1983; Dedkov 2004; Fryirs 2013), small watersheds in the Arctic may cumulatively contribute more sediment to the Arctic Ocean than the large Arctic Rivers.

**Fig. 1.** Map showing (a) the location of Herschel Island and the glaciation limit along the Yukon Coast and (b) the Ice Creek watersheds with the locations for water sampling at the outflow of Ice Creek East (ICE) and Ice Creek West (ICW) and the alluvial fan (AF). Projection: UTM NAD 1983. Image base (b): GeoEye 2011 image.



The knowledge about summer rainfall impacts on the release of DOC, TDS, and SS is limited and few studies report on these dynamics in continuous permafrost areas. The objectives of this paper are therefore to investigate the dynamics of hydrology and hydrochemistry in a small coastal watershed on Herschel Island in the northwestern Canadian Arctic. More specifically, we aim at (1) determining characteristics of discharge associated with baseflow and summer rainfall and at (2) quantifying fluxes of DOC, TDS, and SS with regard to baseflow and rainfall events. The results will contribute to understand how similar watersheds in Low Arctic locations will respond to varying rainfall inputs that become increasingly important in the region (Bintanja and Andry 2017).

### Study site

The Ice Creek West watershed (1.4 km<sup>2</sup>) is located on the eastern coast of Herschel Island at 69.58°N and 138.89°W (Fig. 1). It merges with an adjacent watershed to the east before draining into an alluvial fan and finally into the sea. Herschel Island covers an area of about 116 km<sup>2</sup> with a maximum elevation of 183 m above sea level and is situated in the Beaufort Sea off the Yukon Coast of Canada. The island is an ice-thrust moraine formed by the Laurentide Ice Sheet and it is characterized by the abundance of unconsolidated and fine-grained marine and glacial sediments (Mackay 1959; Pollard 1990; Fritz et al. 2012). The island is situated in the zone of continuous permafrost exhibits high ground

ice contents amounting to 30%–60% of the entire island (Rampton 1982; Pollard 1990; Fritz et al. 2012). Ground temperature monitoring on the east side of the island reveals a mean annual ground temperature of  $-8\text{ }^{\circ}\text{C}$  at zero amplitude depth of approximately 14.5 m (Burn and Zhang 2009).

The island's coast is eroding rapidly and numerous retrogressive thaw slumps associated with the presence of ice-rich permafrost occur along the shore (Lantuit and Pollard 2008; Radosavljevic et al. 2015). Mass wasting also occurs in the form of active layer detachments, thermal erosion gullies, or solifluction on the island and affects the soil organic carbon (SOC) storage (Obu et al. 2017). Smith et al. (1989) classify the soils on Herschel Island based on the Canadian system of soil classification. The island is dominated by organic cryosols, whereas Turbic cryosols (cryoturbation) and static cryosols are present on beaches and spits where near-surface permafrost is absent. The vegetation on Herschel Island is classified as lowland tundra (Smith et al. 1989; Myers-Smith et al. 2011), and can be assigned to subzone E (CAVM Team 2003) or the Low Arctic, respectively. Vegetation cover within the watershed is almost continuous and dominated by *Dryas-graminoid-forb* communities. In the upper flatter sections of the watershed, the landscape is characterized by *Eriophorum vaginatum* tussocks and soils rich in organic matter. Shrubs (*Salix* sp.) up to 1 m in height occur in terrain depressions and the creek confluence. Eroded slopes are quickly recolonized by *Petasites frigidus*, *Artemisia tilesii*, or *Senecio congestus*.

Environment and Climate Change Canada runs an automated weather station at Pauline Cove on Herschel Island (WMO ID: 715010) with temperature recordings since 1995. Records of precipitation are only available since 2004 and are often incomplete. The mean annual air temperature compiled from no-gap data months between 1995 and 2016 is  $-8.4\text{ }^{\circ}\text{C}$  (Environment and Climate Change Canada 2018). Between 1926 and 1970, mean annual air temperatures have been stable in the Canadian western Arctic, followed by a total increase of  $2.7\text{ }^{\circ}\text{C}$  between 1970 and 2005. This increase of temperature is also reflected on Herschel Island where a deepening of the active layer by 15–25 cm has occurred between 1985 and 2005 (Burn and Zhang 2009).

The largest hydrological event of the year is snowmelt, which occurs in late May or early June, where the average monthly air temperatures are  $-3.4$  and  $4.2\text{ }^{\circ}\text{C}$ , respectively. Freeze up of the active layer takes place by mid-November for most of the island (Burn 2012).

## Methodology

### Weather data

During the field monitoring in 2015 and 2016, we installed a weather station in Ice Creek West collecting air temperature (BTF11/002 TSic 506;  $\pm 0.1\text{ }^{\circ}\text{C}$  accuracy), incoming solar radiation (UTK – EcoSens 11.6.6133.0051; error  $< 10\%$ ), wind speed (Thies CLIMA 4.3519.00.173;  $\pm 0.5\text{ m s}^{-1}$  accuracy), and precipitation (tipping bucket gauge Young Model 52203; 0.1 mm per tip; accuracy  $\pm 2\%$ ). Our station was located approximately 1 km away from the station run by Environment and Climate Change Canada.

There is a significant positive correlation ( $R^2 = 0.85$ ;  $p < 0.05$ ) between the two stations (Fig. A1). However, we find that the Environment Canada station underestimates the precipitation by 66% on average compared with our station in Ice Creek West. This may be related to the northwest (NW) wind pattern that is predominant during storms bringing more rain to our weather station in Ice Creek West. The linear regression formula ( $y = 1.28 + 0.42x$ ) has been applied to the Environment Canada data to correct for this offset. We also compared daily mean air temperature between both stations and find a near zero temperature gradient between both, which is why no corrections were applied to the

temperature data. Precipitation data are missing for the complete season of 2014 and also at the stations nearby Komakuk or Shingle Point.

### Hydrology

Discharge was measured during summer months between 2014 and 2016. A cutthroat flume ( $w = 0.2$  m;  $l = 0.7$  m;  $h = 0.5$  m) was equipped with a pulse radar (VEGAPULS WL61;  $\pm 2$  mm accuracy) at a sampling interval of 60 s in 2014, and with a U20 Hobo level logger (U20-001-01;  $\pm 0.05\%$  accuracy) at sampling intervals between 5 min and 2 h in 2015 and 2016. Another Hobo U20 level logger was installed about 3 m upstream in the cross section of the stream to detect and correct deviations during the snow melt period. For compensation of the stage recordings, a third Hobo U20 level logger was secured with rebar close to the discharge station to measure barometric pressure. Discharge was computed based on a standard equation developed by [Skogerboe et al. \(1973\)](#) for the dimensions of the flume. The accuracy for the pulse radar used in 2014 translates to an uncertainty of 20% through error propagation. This accuracy was improved tremendously by updating the equipment to the Hobo U20 level loggers, which show an uncertainty of runoff of 0.3% through error propagation.

In addition to the summer months 2014–2016, data for a full hydrological year is available in 2015/2016 including the snowmelt period. Electrical conductivity (EC) was measured using a Hobo conductivity logger (U24-002-C,  $\pm 5 \mu\text{S cm}^{-1}$ ) located 0.5 m downstream from the cutthroat flume in 2015 and 2016. The sampling interval was adjusted to match the intervals of the Hobo water level loggers between 5 min and 2 h. A Wingscape Pro time-lapse camera (WCT-00121) at 5 min intervals during the summers of 2014 and 2015 and at 3 h intervals during the snowmelt period 2016 were used to monitor the instrumental setup. To analyze separate hydrographs of rainfall events, the subjective method ([Singh 1992](#)) was used to separate baseflow from event flow.

### Suspended sediment and hydrochemistry

An automatic water sampler (ISCO 3700) was used to collect water samples downstream of the flume. In 2014, the sampler was programmed for a 6-h interval starting 31 July at 20:00 and ending 8 Aug. at 14:00. The channel was dried up when monitoring started in 2015, gradually filling with water after rain events. Due to the low water level, manual samples were collected every day around 15:00 between 29 July and 5 Aug. before the automatic water sampler could be installed on 6 Aug. Due to mechanical issues with the device, sampling was irregular in the beginning before the interval was set to 6 h from 7 Aug. until 12 Aug. In 2016, manual samples (1–2 per day) were collected between 20 and 24 July before the automatic water sampler was installed. Samples were taken at a 12-h interval (starting 03:00 on 25 July until 15 Aug.) and more frequently during rainfall events (between 1 and 3 h). In addition to the automated sampling, manual samples were collected at the outflow of Ice Creek East and along the alluvial fan on 30 July 2016 ([Fig. 1](#)). EC and pH were measured in the field within 24 h of sample collection. All samples of 2014 and the majority of samples in 2016 were prepared for hydrochemical analysis directly in the field, whereas samples in 2015 were frozen in 125 mL bottles in the field and analyzed in Germany later. Samples were analyzed for suspended sediment concentration (2015 and 2016), particulate organic carbon (POC) (2016), DOC (2014–2016), dissolved nitrogen (2015 and 2016), and dissolved ions (2014–2016). Along with the stream samples, deionised water used in the field for rinsing of the sampling bottles, was analyzed as blank following the same preparation procedure.

Suspended sediment concentration (SSC) was determined by volumetric vacuum filtration of samples through preweighed and precombusted  $0.7 \mu\text{m}$  glass fiber filters, which were dried at  $50^\circ\text{C}$  for 24 h and subsequently weighed. In 2016, a maximum of 1000 mL was filtered to obtain SSC. Out of the 65 filters from 2016, 36 contained sediment with a

**Table 1.** Summary of total matter fluxes in the monitoring periods and the observed rainfall events and the according matter fluxes.

| Event ID     | Rainfall (mm) | Runoff (mm) | Runoff ratio | Sediment flux (kg km <sup>-2</sup> ) | DOC flux (kg km <sup>-2</sup> ) | TDN flux (kg km <sup>-2</sup> ) | TDS flux (kg km <sup>-2</sup> ) |
|--------------|---------------|-------------|--------------|--------------------------------------|---------------------------------|---------------------------------|---------------------------------|
| 2014_1       | NA            | 10.6        | NA           | NA                                   | 82                              | NA                              | 4040                            |
| 2015_1       | 12.3          | 1.0         | 0.13         | 1120                                 | 6.0                             | 0.6                             | 874                             |
| 2015_2       | 28.1          | 3.0         | 0.09         | 4480                                 | 29                              | 1.6                             | 2170                            |
| 2015_3       | 4.5           | 0.5         | 0.09         | 521                                  | 4.2                             | 0.2                             | 214                             |
| 2016_1       | 33.9          | 3.4         | 0.10         | 254                                  | 40                              | 1.8                             | 1690                            |
| 2016_2       | 9.3           | 0.7         | 0.14         | 14.2                                 | 4.5                             | 0.3                             | 567                             |
| 2016_3       | 12.7          | 0.9         | 0.13         | 46.9                                 | 6.2                             | 0.4                             | 725                             |
| 2014 (total) | NA            | 6.9         | NA           | NA                                   | 120                             | NA                              | 6670                            |
| 2015 (total) | 40.8          | 6.6         | 0.06         | 7250                                 | 50                              | 3.0                             | 3680                            |
| 2016 (total) | 56.4          | 8.0         | 0.07         | 360                                  | 75                              | 4.0                             | 5400                            |

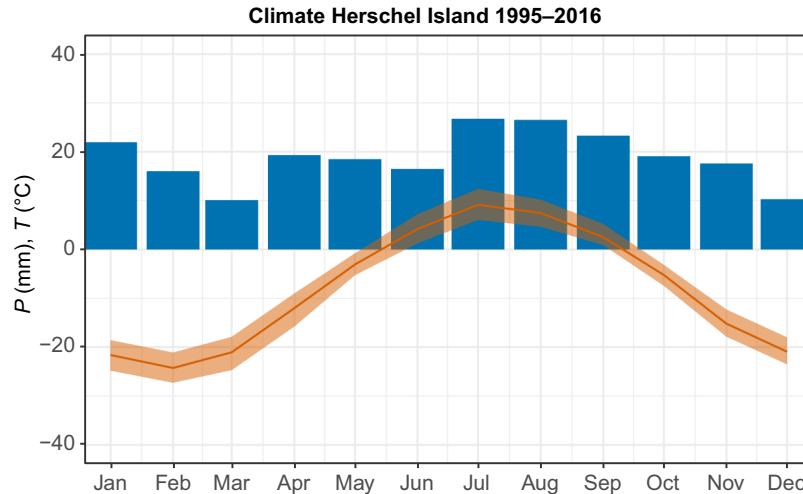
Notes: Rainfall, runoff, runoff ratio, sediment, dissolved organic carbon (DOC), total dissolved nitrogen (TDN), and total dissolved solids (TDS) fluxes (in kg km<sup>-2</sup>) are reported for every rain event. NA, not available.

minimum net weight of 10 mg. These were ground using a mortar to homogenize the filter-sample mixture. Inorganic carbon was removed prior to duplicate measurements of 6 mg each in an elemental analyzer (Flash 2000, Thermo Scientific, Germany) to obtain C<sub>org</sub> (%). This procedure was also carried out for two blank filters to account for a possible signal from the filters. Based on the net weights of filter and sample, and the filtered volume, POC concentrations in the suspended material (%) and POC concentrations in the water (mg L<sup>-1</sup>) were calculated.

Samples for DOC and dissolved nitrogen (TDN) analyzes were acidified with HCl (30% suprapur) prior to the measurements. In 2014, a Shimadzu TOC-VCPH analyzer was used to determine DOC, whereas a Shimadzu TOC-L analyzer with a TNM-L module was used for the 2015–2016 samples to determine DOC and TDN. Inorganic carbon (TIC) was sparged out with synthetic air prior to the measurement. In 2016, there was a shortage of HCl in the field, hence 82 samples were frozen and acidified upon return. Once new acid was acquired, duplicates of 48 samples were frozen and acidified to determine the effect of different sample treatment. We find a significant linear relationship ( $p < 0.05$ ;  $n = 47$ ) between DOC concentrations of unfrozen and frozen samples with an  $R^2$  of 0.87 (Fig. A2). Samples that were frozen in the field, thawed and acidified in the lab result in lower concentrations (on average by 13% of the unfrozen samples) than samples that were acidified directly in the field and remained unfrozen. The periods of different sample treatment are indicated in the data. Concentrations for TDN were below detection limit ( $<0.45$  mg L<sup>-1</sup>) for the frozen samples, which makes a similar comparison impossible.

Samples for the anion and cation analysis were filtered through a cellulose acetate membrane syringe prefilter with a pore size of 0.45  $\mu$ m. Cation samples were conserved with 65% HNO<sub>3</sub> (65% suprapur). Due to the lack of sufficient acid, 82 cation subsamples were frozen and later conserved upon return to Germany in 2016. A Perkin Elmer Optima 3000XL ICP-OES spectrometer was used to determine dissolved cations Al<sup>+</sup>, Ba<sup>2+</sup>, Fe, Mn, Sr<sup>2+</sup> (in  $\mu$ g L<sup>-1</sup>), Ca<sup>2+</sup>, K<sup>+</sup>, Mg<sup>2+</sup>, Na<sup>+</sup>, P, and Si<sup>4+</sup> (in mg L<sup>-1</sup>). To determine dissolved anions F<sup>-</sup>, Cl<sup>-</sup>, SO<sub>4</sub><sup>2-</sup>, Br<sup>-</sup>, NO<sub>3</sub><sup>-</sup>, and PO<sub>4</sub><sup>3-</sup> (in mg L<sup>-1</sup>), analyzes were performed on a Dionex DX-320 ion chromatograph. The concentration of HCO<sub>3</sub><sup>-</sup> (mg L<sup>-1</sup>) was determined on a Metrohm Titrino 794 titrator. TDS reported in this study are the sum of all dissolved anions and cations. Concentrations below the detection limit were reported in Table 1, and set to the detection limit for statistical analysis. The charge balance error was computed following Freeze and Cherry (1979), resulting in a mean of 1.23% and remaining below 9.62% for all the samples.

**Fig. 2.** Climatic conditions retrieved from the automated weather station on Herschel Island between 1995 and 2016 including only months with no data gaps (Environment and Climate Change Canada 2018). The plot shows minimum, maximum, and mean temperatures  $T$  (orange line and ribbon in °C) and precipitation  $P$  (blue in mm).



### Flux estimates and statistics

To obtain flux estimates for parameter  $F_p$ , mean runoff volume  $\bar{Q}$  during every time step  $t$  was multiplied with the concentration of the parameter  $[P]_t$  at that time. The flux estimates are summed for the time interval of interest  $t_n$  (Eq. 1).

$$(1) \quad F_p = \sum_{t_0}^{t_n} (\bar{Q} \times [P]_t)$$

The mean runoff volume  $\bar{Q}$  for a time interval of interest  $t_n$  is the mean of all discharge runoff values from half the interval before and after  $t_n$  (Eq. 2). For example, if the interval is 6 h, the mean is computed from 3 h until 9 h.

$$(2) \quad \bar{Q} = n^{-1} \sum_{t_0 - \frac{t_n}{2}}^{t_n + \frac{t_n}{2}} Q_t$$

Statistical tests used in this study were performed with RStudio (Version 1.0.153). Normality of distributions was tested using the Shapiro–Wilk normality test. The student's  $t$  test was used to compare the means of parameters between for example different years. If the distribution was not normally distributed, the Wilcoxon Rank-Sum Test was applied. To test the correlation between two variables, the Pearson correlation coefficient was used.

## Results

### Meteorological conditions

The mean annual air temperatures were  $-7.4$  °C in 2014 and  $-6.3$  °C in 2016 (Fig. 2) and therefore higher compared with the available climate record between 1995 and 2016 ( $-8.4$  °C). The monthly air temperatures varied, with generally higher temperatures in the winter months compared with the long-term averages. The mean monthly air temperatures (1995–2016) for the monitoring months July and August were  $9.0$  and  $7.3$  °C, respectively. Whereas the years of 2014 and 2015 showed mean monthly air temperatures of  $9.1$  and

7.8 °C for July and 6.8 and 7.1 °C for August, the year of 2016 exhibited higher air temperatures in both months (9.4 and 7.7 °C). Snowmelt typically occurs in May. The mean monthly air temperatures for May 2014 and 2016 showed higher values (−1.2 and −0.1 °C) compared with the mean (−3.4 °C). Temperature data is unavailable for May 2015.

Rainfall for the monitoring period of 2015 (17 days) was 48 mm, and 47 mm for the monitoring period of 2016 (22 days). No precipitation data for Herschel Island or the closest climate stations is available for 2014. Due to this lack of consistent precipitation records, it was impossible to determine the climatic conditions comprehensively before the monitoring started.

### Streamflow and EC

The major hydrological event during the year is the melting of snow in the spring. Peak flow reached  $0.377 \text{ m}^3 \text{ s}^{-1}$  on 14 May 2016 (Fig. A3). Photos from the time-lapse camera show a change in the snow wetness and ponding 2 days prior to the initiation of flow (Appendix B).<sup>1</sup> The high flow declined rapidly to  $0.048 \text{ m}^3 \text{ s}^{-1}$  within 6 days, and a diel pattern was visible from week 21 onwards. A diel flow regime is characterized by higher stream discharge during daytime where remaining snow patches melt under the incoming solar radiation. The amount of precipitation during that time was not high enough to alter this diel flow pattern and appeared to have a minor contribution to the water flow in the stream. As time progressed, the peak runoff during the day was shifted earlier; it occurred at 20:30 during week 21 and at 18:30 during week 24. Also, the amplitude decreased as snow left the catchment as runoff. From mid-June onwards (week 25), this pattern faded out indicating that melting of snow patches did no longer control the baseflow of the creek. EC rose exponentially from below  $10 \text{ } \mu\text{S cm}^{-1}$  at the onset of snowmelt in 2016 to around  $300 \text{ } \mu\text{S cm}^{-1}$  in mid June and it did not follow a diel pattern (Fig. A3). This period is termed nival recession.

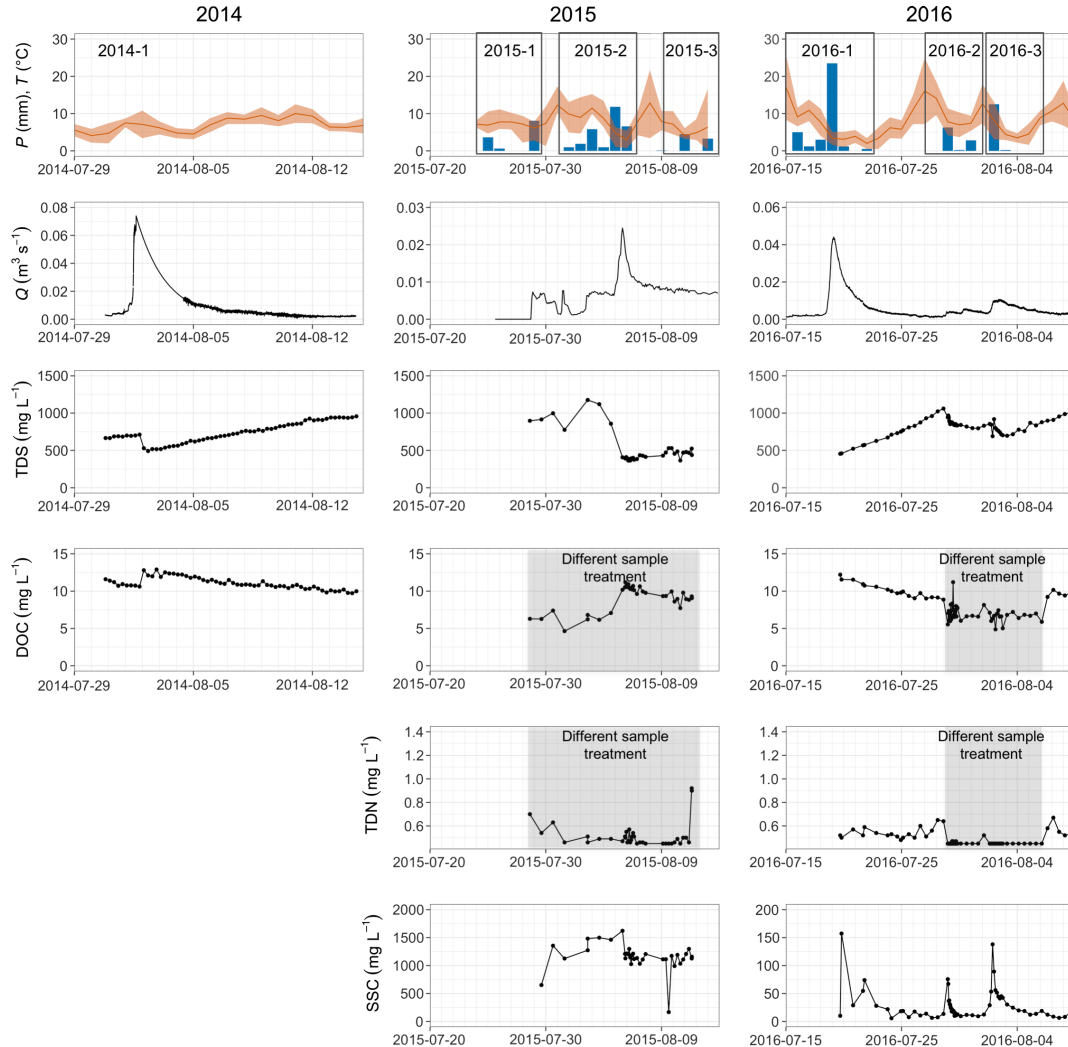
From the end of June 2016 onwards, baseflow was controlled by rainfall events. We observed a total of seven rainfall events of different magnitudes in 2014, 2015, and 2016 (Fig. 3). Maximum flows recorded in the summer 2014–2016 were  $0.024 \text{ m}^3 \text{ s}^{-1}$  in 2015,  $0.044 \text{ m}^3 \text{ s}^{-1}$  in 2016, and  $0.074 \text{ m}^3 \text{ s}^{-1}$  in 2014. This is substantially lower than flows that can be expected during spring freshet. In all 3 years of monitoring, the catchment responded quickly to the input of rain as indicated by linear rising hydrographs and the quick returns to baseflow conditions (Fig. 3). EC decreased with rising hydrographs and recovered thereafter. It reached maximum during the summer, up to  $2000 \text{ } \mu\text{S cm}^{-1}$  as in July 2015. This period is referred to as baseflow/stormflow period. Rainfall to runoff ratios ranged between 0.09 and 0.14; 2015 being slightly less efficient in water export than 2016 (Table 1). As visible in the hydrographs throughout the years, baseflow rises with rainfall events (Fig. 3).

### Transport of suspended sediment and organic matter

The transport of suspended sediment varied significantly ( $p < 0.05$ ) between both years of available summer data in 2015 and 2016 (Fig. 4; Table A1). The mean suspended sediment concentration was  $1180 \text{ mg L}^{-1}$  in 2015 and  $28.2 \text{ mg L}^{-1}$  in 2016, with minima of  $167.5 \text{ mg L}^{-1}$  (2015) and  $5.7 \text{ mg L}^{-1}$  (2016), respectively (Table A2). Sediment and discharge hysteresis (Fig. 5) suggest a rapid initial mobilization of sediments during rainfall events followed by an exhaustion expressed as clockwise hysteresis loops. Peaks in sediment concentration were often reached before discharge peaked. The total sediment flux over the season amounted  $7245 \text{ kg km}^{-2}$  in 2015 and  $360 \text{ kg km}^{-2}$  in 2016. When looking at sediment export

<sup>1</sup>Supplementary material is available with the article through the journal Web site at <http://nrcresearchpress.com/doi/suppl/10.1139/as-2018-0010>.

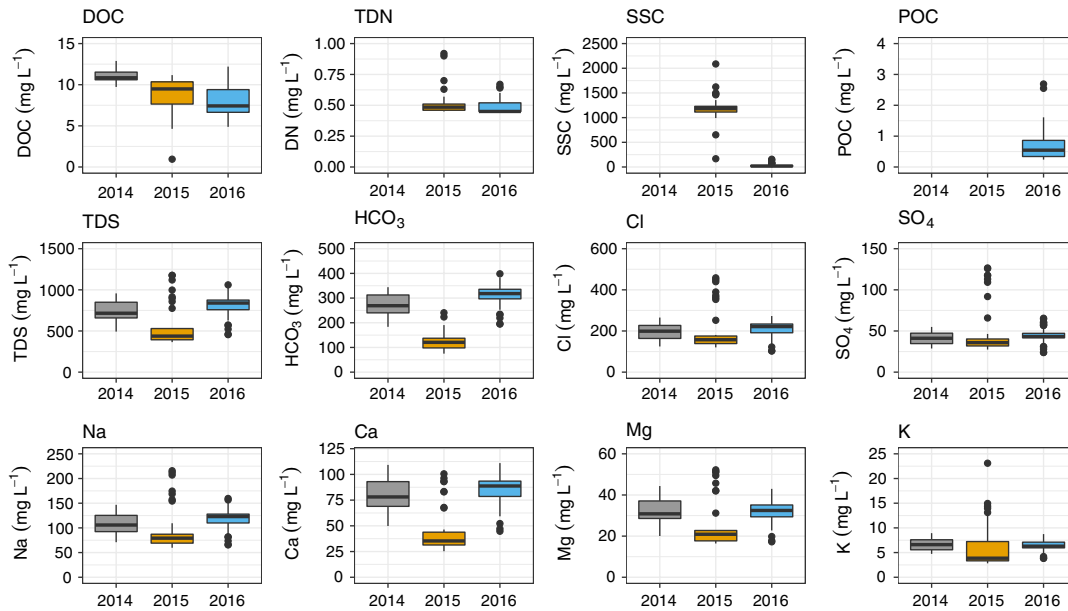
**Fig. 3.** Summary plot showing minimum, maximum and mean temperatures  $T$  (orange line and ribbon in  $^{\circ}\text{C}$ ), precipitation  $P$  where available (blue in mm), discharge ( $\text{m}^3 \text{s}^{-1}$ ), total dissolved solids (TDS), dissolved organic carbon (DOC), total dissolved nitrogen (TDN), and suspended sediment concentration (SSC) (all in  $\text{mg L}^{-1}$ ) for the monitoring seasons 2014, 2015, and 2016. The rain events labels are indicated in the upper plots. Note that differences in sample treatment for DOC and TDN samples are indicated in the plots in grey. Values below the detection limit were set to the value of the detection limit.



in relation to water flux (Fig. 6a), event 2016-1 stands out because of its very low sediment flux. This result should be treated with caution, because the estimate is only based on available samples capturing the falling limb of the hydrograph. The high sediment pulse is likely to have occurred on the rising limb already.

POC values varied between  $0.24$  and  $2.69 \text{ mg L}^{-1}$ , with a mean of  $0.75 \pm 0.58 \text{ mg L}^{-1}$ . The carbon content of the suspended sediment ranged between  $1.4\%$  and  $3.3\%$  with a mean of  $2.0 \pm 0.004\%$ . Mean DOC concentrations were  $11.1 \pm 0.8 \text{ mg L}^{-1}$  in 2014,  $8.8 \pm 2.1 \text{ mg L}^{-1}$  in 2015, and  $8.0 \pm 4.9 \text{ mg L}^{-1}$  in 2016. The DOC concentrations between all years differed significantly ( $p < 0.05$ ; Table A1). Values for total dissolved nitrogen (TDN) ranged between  $0.5$  and  $0.9 \text{ mg L}^{-1}$  in 2015, and  $0.5 \text{ mg L}^{-1}$ , and  $0.7 \text{ mg L}^{-1}$  in 2016 (Table A2), being significantly

**Fig. 4.** Boxplots showing hydrochemical concentrations of dissolved organic carbon (DOC), total dissolved nitrogen (TDN), suspended sediment concentration (SSC), particulate organic carbon (POC), total dissolved solids (TDS), and major ions at the outflow of Ice Creek West for 2014 (grey), 2015 (orange), and 2016 (blue). Note that values below the detection limit were set to the value of the detection limit. Boxplots for the remaining measured ions are found in Figure A4.



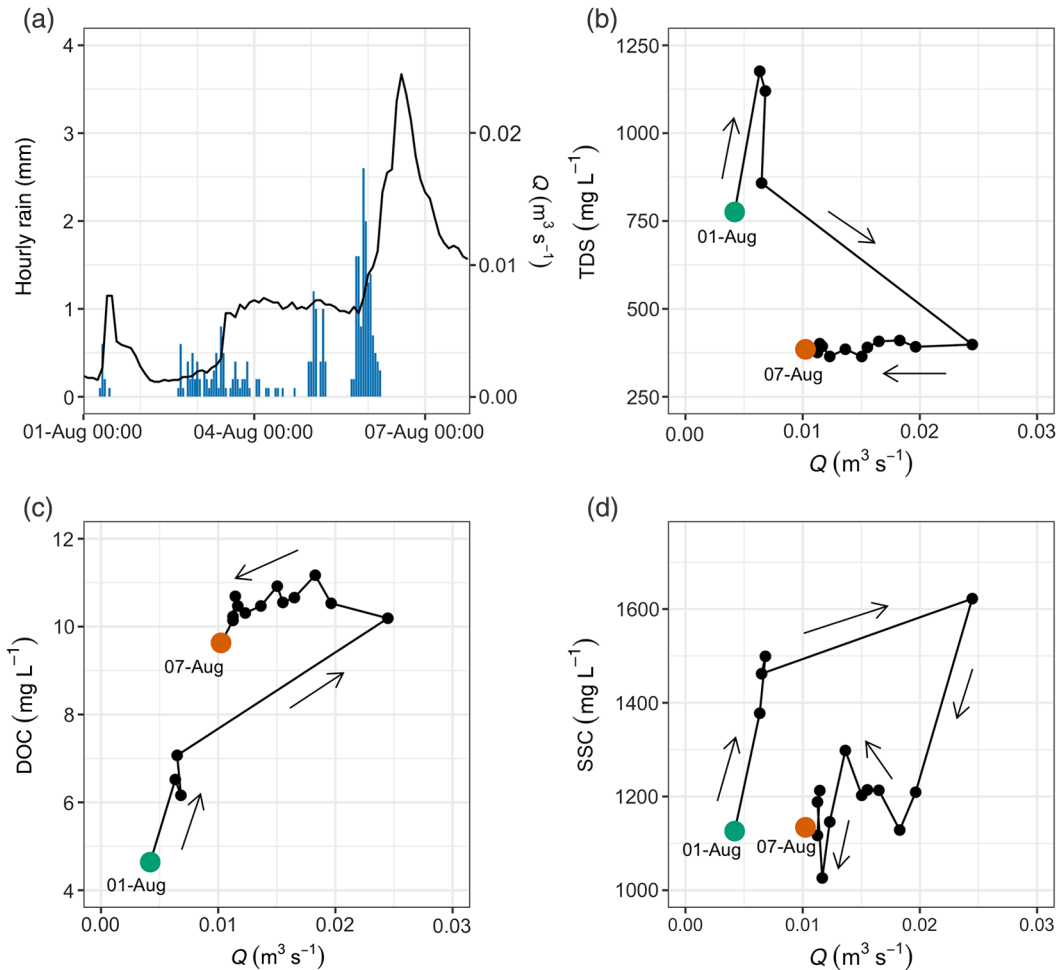
different from each other ( $p < 0.05$ ). DOC shows a clear response to rainfall events, with increasing concentrations as flow increases (Fig. 5). DOC concentrations are commonly still rising after peak discharge; therefore, the hysteresis loop is counter-clockwise. The total DOC output was  $123.5 \text{ kg km}^{-2}$  in 2014,  $49.6 \text{ kg km}^{-2}$  in 2015, and  $74.9 \text{ kg km}^{-2}$  in 2016. The TDN output was very low with  $3.0 \text{ kg km}^{-2}$  in 2015 and  $4.0 \text{ kg km}^{-2}$  in 2016 (Table 1). The relationship between water flux and output of DOC and TDN (Figs. 6b, 6c) is very strong ( $R^2_{\text{DOC}} = 0.99$ ;  $R^2_{\text{TDN}} = 0.99$ ;  $p < 0.05$ ). Whereas we find a strong positive relationship ( $R^2 = 0.99$ ;  $p < 0.05$ ) between concentrations of POC and SSC (Fig. 7a), there is no clear relationship between SSC and DOC, POC and DOC, or SSC and TDS (Fig. 7).

#### Solute transport

The mean concentration of TDS — the summation of anions and cations — was  $738 \pm 134 \text{ mg L}^{-1}$  in 2014,  $553 \pm 247 \text{ mg L}^{-1}$  in 2015, and  $815 \pm 121 \text{ mg L}^{-1}$  in 2016 (Table A2). The concentrations differed significantly between the years with the lowest average and greatest variability (between 365 and 1176  $\text{mg L}^{-1}$ ) observed in 2015. Decrease of TDS concentrations with increasing runoff during rainfall events was indicated by a clockwise hysteresis loop (Fig. 5). There is a strong positive relationship between water flux and TDS export (Fig. 6d) for all individual rainfall events ( $R^2 = 0.99$ ;  $p < 0.05$ ).

The major ions contributing to the sum of TDS were (highest to lowest) bicarbonate, chloride, sodium, calcium, sulfate, and magnesium (Fig. 4). All ions show a similar pattern as TDS with lower mean values in 2015, some of them being significant (Appendix A). We find that the outliers outside the fourth quartile occur just after the initiation of flow at the beginning of monitoring in 2015. Examining the hydrochemical facies in a piper diagram (Fig. 8) reveals that the composition of the water in 2015 differed from the other

**Fig. 5.** Catchment response to 28.1 mm rainfall event 2015-2 (1–7 Aug.). (a) Rainfall and hydrograph response, (b) discharge–TDS hysteresis, (c) discharge – DOC hysteresis, and (d) discharge–SSC hysteresis. The hysteresis line follows every time step from the beginning (green dot) to the end (red dot) of the rainfall event, and the direction is indicated by the arrows. Hysteresis patterns for all recorded rain events can be found in the Figures A5 and A6.

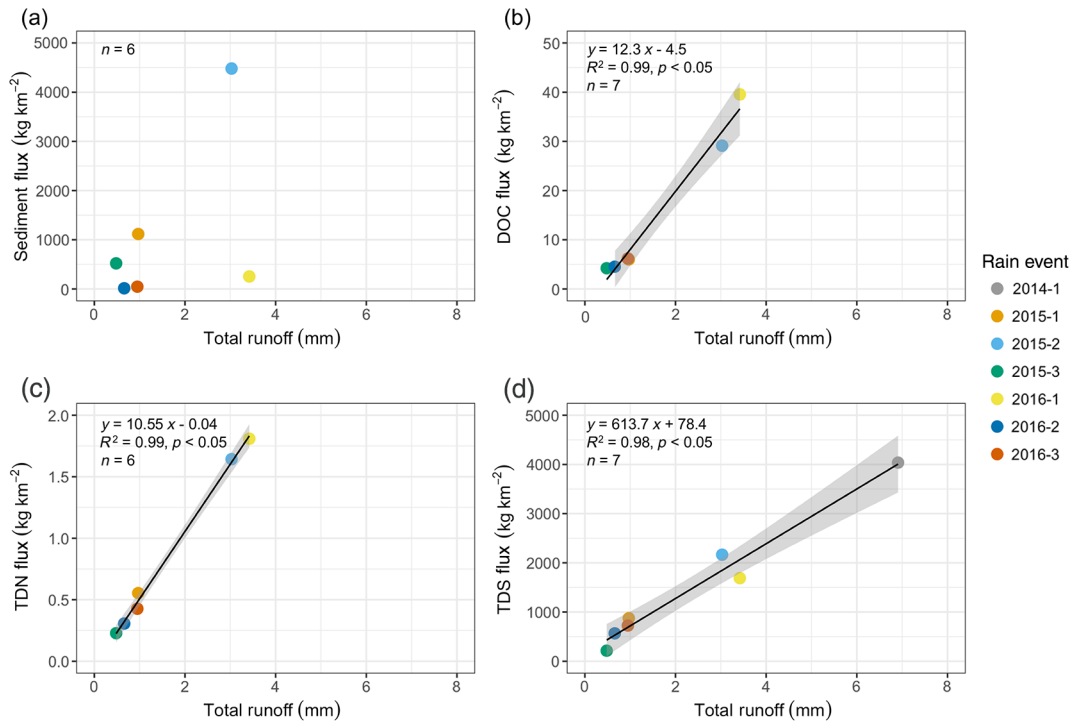


2 years. Whereas in 2014 and 2016, the water type was mixed with no dominant facies, the composition shifts towards sodium chloride type in 2015. Compared with the other years, we find higher chloride concentrations and a slight decline in alkalinity in 2015. The total TDS output amounted  $6670 \text{ kg km}^{-2}$  in 2014,  $3680 \text{ kg km}^{-2}$  in 2015, and  $5400 \text{ kg km}^{-2}$  in 2016 (Table 1).

#### Alluvial fan sampling

Results from sampling the outlets draining from the alluvial fan into the Beaufort Sea on 30 July 2016 are presented in Table 2, together with concentrations at the outflow from Ice Creek East and West at the same day. Suspended sediment concentrations were highly variable with  $53.5 \text{ mg L}^{-1}$  (POC:  $4.0 \text{ mg L}^{-1}$ ) at location AF#2 and only  $0.7 \text{ mg L}^{-1}$  at location AF#5. Both locations are very close to each other on the eastern side of the alluvial fan (Fig. 1). DOC concentrations were very similar to the ones recorded at the outflow of the

**Fig. 6.** Relation between total runoff and (a) sediment flux, (b) dissolved organic carbon (DOC) flux, (c) total dissolved nitrogen (TDN) flux, and (d) total dissolved solids (TDS) flux for all recorded rainfall events. All fluxes are reported in  $\text{kg km}^{-2}$ . The ribbon around the regression line indicates the standard error.



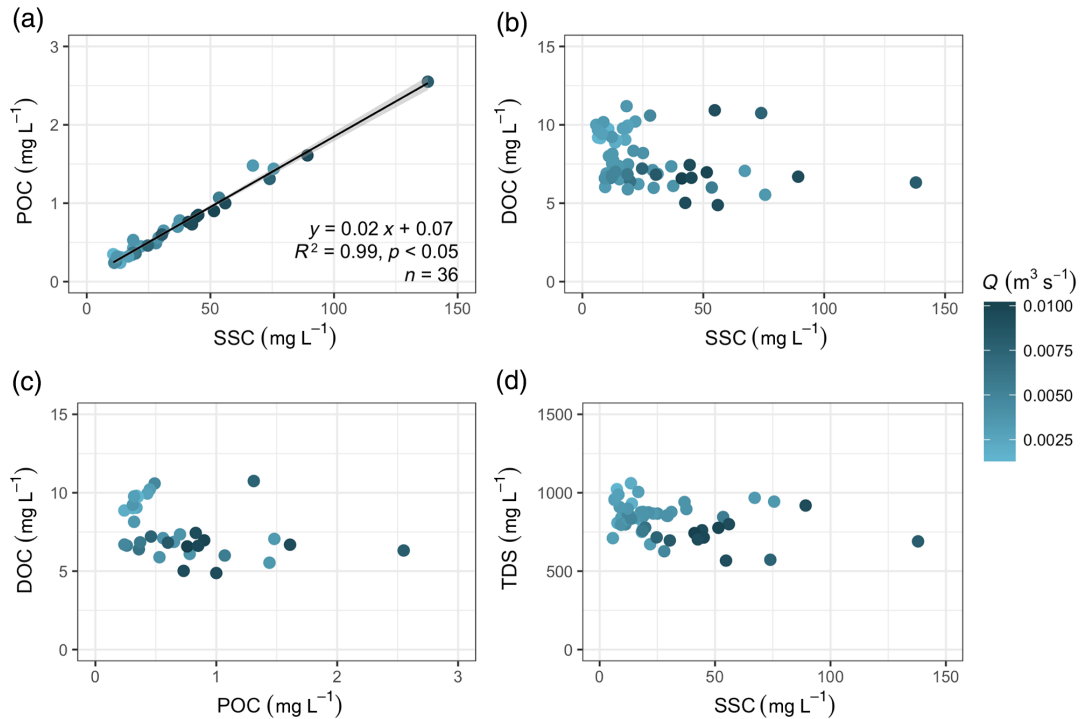
Ice Creek East and West ( $5.7$  and  $7.7 \text{ mg L}^{-1}$ ). They ranged between  $4.7 \text{ mg L}^{-1}$  at AF#6 and  $8.1 \text{ mg L}^{-1}$  at AF#3. TDN concentrations remained below the detection limit of  $0.45 \text{ mg L}^{-1}$  for all sampling points. Concentrations of TDS were slightly lower after draining through the alluvial fan, ranging between  $268.0 \text{ mg L}^{-1}$  at AF#6 and  $448.9 \text{ mg L}^{-1}$  at AF#2.

## Discussion

### Hydrological response

The Ice Creek West watershed exhibits a typical nival flow regime, where snowmelt is the largest hydrological event of the year. Thawing of permafrost and melting of ground ice alone during the summer does not seem to generate substantial runoff. Therefore, summer baseflow is controlled by rainfall events and remains very low compared with the post nival recession. Watershed conditions prior to rainfall events have an effect on the runoff response. When monitoring started in 2015, there was no runoff at all in Ice Creek West, which points towards very dry conditions prior to that period. Although we do not have climate data to support this, there was presumably only little to no rain in the weeks prior to onset of monitoring. The  $4.2 \text{ mm}$  of rain during the 25th and 26th July did not generate flow. Only after the  $8.1 \text{ mm}$  rainfall event 3 days later, the catchment responded and the stream was activated. In contrast, rain events 2015-3 with  $4.5 \text{ mm}$  and 2016-3 with  $12.7 \text{ mm}$  occurred late in the season and did not show any discernible impact on the hydrograph. This shows that baseflow increases as more rainfall events occur during the late summer season. This finding is very typical for environments where water infiltration is impeded by the permafrost table (Woo 2012). The hydrological response is directly

**Fig. 7.** Scatterplots showing the relation between (a) suspended sediment concentration (SSC) and particulate organic carbon (POC), (b) SSC and dissolved organic carbon (DOC), (c) POC and DOC, and (d) SSC and total dissolved solids (TDS) for the year of 2016. Concentrations are in  $\text{mg L}^{-1}$ . The colour of each point indicates the discharge ( $\text{m}^3 \text{s}^{-1}$ ) at the time the sample was collected. The ribbon around the regression line in (a) indicates the standard error.



resulting in a sharply rising hydrograph, followed by an elongated falling limb. This is expected for a small catchment size of  $1.4 \text{ km}^2$ . The runoff ratios are in a similar range for all rainfall events (mean = 0.11) indicating inefficient water routing and high water storage capacity in the watershed. If we assume a similar runoff ratio for 2014, we estimate the amount of rain to be roughly 76 mm based on the measured water flux. This would mean that the 2014 rain event was the greatest of all monitored years. Favaro and Lamoureux (2014) find a high range of runoff ratios between 0.001 and 0.84 in a  $8.0 \text{ km}^2$  watershed (West River) at Cape Bounty, Melville Island in the High Arctic depending on the soil moisture conditions in the catchment. Carey et al. (2013) also find runoff ratios between 0.29 and 0.66 in a  $7.6 \text{ km}^2$  alpine headwater stream (Granger Basin) in the discontinuous permafrost zone. High runoff ratios indicate saturated antecedent conditions and thus, more efficient water routing. Projections for the Arctic show an increase of summer precipitation (Bintanja and Andry 2017), which would in turn, also lead to an increase in summer flow. Although the changes observed are not being significant, we find a decrease in drainage efficiency expressed through the runoff ratio later in the season (Table 1). This may reflect the deepening of the active layer, which increases the water storage capacity of the catchment.

#### Water quality and fluxes

DOC flux varies significantly between  $124 \text{ kg km}^{-2}$  in 2014 and  $49.6 \text{ kg km}^{-2}$  in 2015 (Table 1). The year of 2016 shows significantly higher DOC concentrations and flux ( $74.9 \text{ kg km}^{-2}$ ) compared with 2015. These values need to be treated with caution as samples

**Fig. 8.** Piper diagram showing the composition of major anions and cations at the outflow of Ice Creek West for 2014 (grey), 2015 (orange), and 2016 (blue).

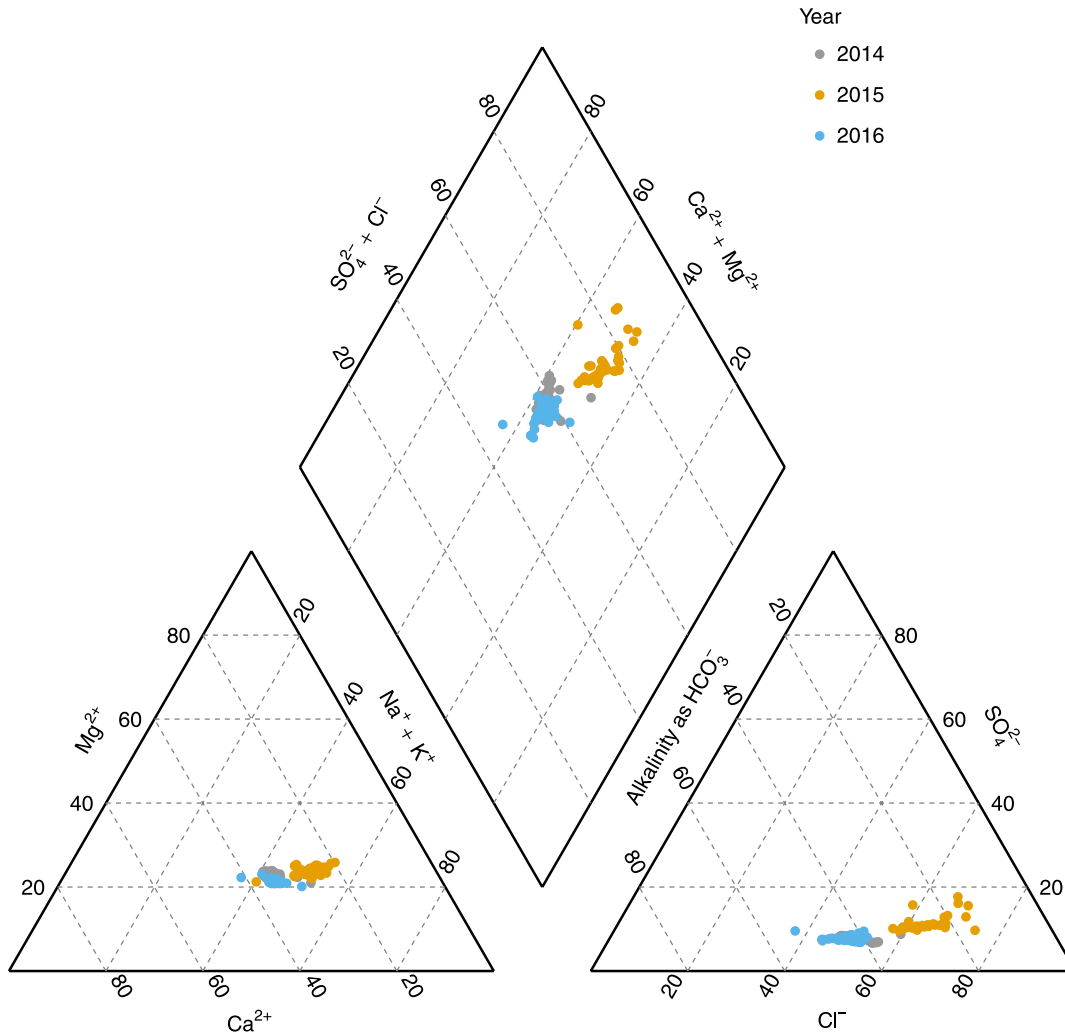


**Table 2.** Concentrations of suspended sediment (SS), dissolved organic carbon (DOC), total dissolved nitrogen (TDN), total dissolved solids (TDS), and particulate organic carbon (POC) (all in  $\text{mg L}^{-1}$ ) from Ice Creek West and the adjacent Ice Creek East as well as from outflows along the alluvial fan on 30 July 2016.

| Location       | SS<br>( $\text{mg L}^{-1}$ ) | DOC<br>( $\text{mg L}^{-1}$ ) | TDN<br>( $\text{mg L}^{-1}$ ) | TDS<br>( $\text{mg L}^{-1}$ ) | POC<br>( $\text{mg L}^{-1}$ ) | Number of<br>samples |
|----------------|------------------------------|-------------------------------|-------------------------------|-------------------------------|-------------------------------|----------------------|
| Ice Creek East | 3.8                          | 5.7                           | <0.45                         | 490.0                         | NA                            | 1                    |
| Ice Creek West | 12.7                         | 7.7                           | <0.45                         | 519.2                         | NA                            | 1                    |
| AF#1           | 12.0                         | 5.5                           | <0.45                         | 332.8                         | NA                            | 1                    |
| AF#2           | 53.5                         | 6.6                           | <0.45                         | 448.9                         | 4.0                           | 1                    |
| AF#3           | 25.1                         | 8.1                           | <0.45                         | 455.7                         | 1.6                           | 1                    |
| AF#4           | 3.2                          | 6.7                           | <0.45                         | 433.8                         | NA                            | 1                    |
| AF#5           | 0.7                          | 5.1                           | <0.45                         | 416.2                         | NA                            | 1                    |
| AF#6           | 5.8                          | 4.7                           | <0.45                         | 268.0                         | NA                            | 1                    |

Notes: NA, not available.

in 2015 and partly in 2016 were treated differently, and thus, may underestimate DOC concentration and flux (see “Suspended sediment and hydrochemistry” section for more details). We observe an increase of DOC export with increasing water flux (Fig. 6), which strongly suggests that DOC export is controlled by rainfall in our study site. Projected increase of discharge in the future (Bintanja and Andry 2017) may lead to higher DOC fluxes from the catchment.

Flux estimates for DOC have been reported for a number of locations across the Arctic (Table 3). For more adequate comparison, values from other studies were scaled down to 17 days of flux, i.e., the average monitoring period in this study. At Ice Creek West, we estimate the mean flux to be  $82.7 \pm 30.7 \text{ kg km}^{-2}$  over all 3 years of monitoring (17 days in the summer). This value is higher than the DOC flux reported from the High Arctic, such as from Melville Island ( $1.6\text{--}25.7 \text{ kg km}^{-2}$ ) by Fouché et al. (2017) or Cornwallis Island ( $7.4 \text{ kg km}^{-2}$ ) by Semkin et al. (2005). The availability of DOC is different between Low Arctic and High Arctic due to differences in vegetation cover. DOC fluxes are also reported from subarctic sites, such as Alaskan catchments with different permafrost coverage ( $18.8\text{--}43.5 \text{ kg km}^{-2}$ ) by Petrone et al. (2006) and Granger Basin in the Yukon territory ( $28.6 \text{ kg km}^{-2}$ ) by Carey (2003). These catchments drain areas of discontinuous permafrost and range below  $10 \text{ km}^2$  in size. Flow pathways in those locations are possibly deeper, and may lead to less mobilization of DOC compared with our study site. The Mackenzie River, which is estimated to transport  $50.2 \text{ kg km}^{-2}$  during a 17-day summer period, is a large Arctic River including areas of sporadic and without permafrost. Flux estimates from boreal watersheds in Sweden with no permafrost coverage ( $79.8\text{--}210.7 \text{ kg km}^{-2}$ ) by Laudon et al. (2004) are much greater than those found in our study. Flux estimates for DOC (mean =  $1756.9 \text{ kg km}^{-2}$ ) have also been provided by Weege (2016) for an outlet stream of a retrogressive thaw slump nearby our study site over two summer monitoring periods. This value exceeds the other DOC yields greatly and might reflect the heavy disturbance associated with that location. Disturbances and thermokarst need to be taken into account when creating flux budgets. Holmes et al. (2012) provide the cumulative DOC flux for all six large Arctic Rivers, amounting  $91.0 \text{ kg km}^{-2}$  for a 17-day summer period. Hence, our estimate is within the same range highlighting the relative importance of small watersheds in terms of DOC flux to the Arctic Ocean. Only rough estimates for the unmonitored circum-Arctic region are provided by (Holmes et al. 2012) assuming same aerial yields for the unmonitored watersheds. Comparing our Low Arctic flux estimates to other studies in the Subarctic and High Arctic highlights the spatial variability of fluxes across latitudes. This will be of importance for future upscaling efforts. Besides riverine fluxes, coastal erosion including mobilization of ground ice might contribute to the DOC flux budget (Fritz et al. 2015). Tanski et al. (2016) estimated the DOC flux in ground ice mobilized through coastal erosion along the Yukon Coast to be  $54\,900 \pm 900 \text{ kg yr}^{-1}$ . This shows that rivers and thaw streams are a much larger contributor of DOC to the coastal zone.

It is important to remember that this study is constrained to monitoring periods (on average 17 days) in the summers of 2014–2016. Comparing those values to the literature is very simplified and does not take into account any temporal variations from those sites (e.g., stormflow events). Further, as studies across the Arctic show, snowmelt as the major hydrological event, plays an important role for water quality and DOC flux in particular. Petrone et al. (2006) find that 45% of DOC is transported during snowmelt, Laudon et al. (2004) find 50%–68% in boreal Sweden, and Fouché et al. (2017) reported 76%–99% for the same runoff period in the High Arctic. Our monitoring needs to be extended capturing the full hydrological year including the snowmelt period.

The suspended sediment (SS) export varies strongly between the years although the measured total runoff remains similar (6.6 mm in 2015 and 8.0 mm in 2016). The year of 2015

**Table 3.** Annual, summer, and 17-days dissolved organic carbon (DOC) fluxes from different Arctic locations sorted by the 17-day DOC yield.

| Catchment                   | Study                   | Area                       | Watershed (km <sup>2</sup> ) | 17-day DOC yield (kg km <sup>-2</sup> ) | Summer DOC yield (kg yr <sup>-1</sup> km <sup>-2</sup> ) | Annual DOC yield (kg yr <sup>-1</sup> km <sup>-2</sup> ) |
|-----------------------------|-------------------------|----------------------------|------------------------------|---|--|--|
| ALD                         | Fouché et al. 2017      | Melville Island, Nunavut   | 0.3                          | 1.6                                     | 4  | 110  |
| Caribou                     | Fouché et al. 2017      | Melville Island, Nunavut   | 0.3                          | 1.9                                     | 5  | 420  |
| Amituk Lake catchment       | Semkin et al. 2005      | Cornwallis Island, Nunavut | 26.5                         | 7.4 <sup>a</sup>                        | NA   | 160  |
| CPCRW low                   | Petrone et al. 2006     | Alaska                     | 5.3                          | 18.8                                    | 152  | 430  |
| Goose                       | Fouché et al. 2017      | Melville Island, Nunavut   | 0.2                          | 24.4                                    | 57   | 870  |
| Ptarmigan                   | Fouché et al. 2017      | Melville Island, Nunavut   | 0.2                          | 25.7                                    | 60   | 260  |
| CPCRW medium                | Petrone et al. 2006     | Alaska                     | 10                           | 27.7                                    | 223  | 530  |
| Granger Basin               | Carey 2003              | Yukon Territory            | 6                            | 28.6                                    | 541  | 1640   |
| CPCRW high                  | Petrone et al. 2006     | Alaska                     | 5.7                          | 43.5                                    | 350  | 830  |
| Mackenzie                   | Holmes et al. 2012      | Mackenzie River            | 1.68 × 10 <sup>6</sup>       | 50.2                                    | 363  | 820  |
| Sörbacken                   | Laudon et al. 2004      | Northern Sweden            | 62                           | 79.8                                    | 432  | 4800   |
| Ice Creek West <sup>b</sup> | This Study <sup>a</sup> | Yukon Coast                | 1.4                          | 82.7 ± 30.7                             | NA   | NA   |
| Västrabacken                | Laudon et al. 2004      | Northern Sweden            | 0.1                          | 99.8                                    | 540  | 3600   |
| Lillan                      | Laudon et al. 2004      | Northern Sweden            | 21                           | 118.3                                   | 640  | 6400   |
| Stridbäcken                 | Laudon et al. 2004      | Northern Sweden            | 9                            | 122.9                                   | 665  | 3500   |
| Mellansjöbacken             | Laudon et al. 2004      | Northern Sweden            | 26                           | 131.9                                   | 714  | 5100   |
| Kallkalsbacken              | Laudon et al. 2004      | Northern Sweden            | 0.5                          | 180.3                                   | 976  | 6100   |
| Kallkalstmyrn               | Laudon et al. 2004      | Northern Sweden            | 0.2                          | 210.7                                   | 1140   | 7600   |
| Slump D                     | Weege 2016              | Yukon Coast                | 0.1                          | 1756.9                                  | NA   | NA   |
| Arctic Rivers               | Holmes et al. 2012      | Circum-Arctic              | 1.09 × 10 <sup>7</sup>       | 91.0                                    | 658  | 1670   |

**Note:** ALD, active layer detachment (catchment); CPCRW, Caribou Poker Creeks Research Watershed. This 17-day DOC yield was scaled down from summer DOC yields to make values from Ice Creek West comparable. Numbers from the literature were reduced to significant digits. NA, not available.

<sup>a</sup>No summer estimate was available for this location, which is why the 17 d DOC yield is based on the entire year.

<sup>b</sup>Mean of DOC fluxes recorded during the monitoring periods of the summers 2014, 2015, and 2016.

shows a significantly higher sediment yield ( $7245 \text{ kg km}^{-2}$  compared with  $360 \text{ kg km}^{-2}$  in 2016), which is most likely caused by a short-lived sediment supply. No major permafrost disturbances have been observed during that time, which leads to the hypothesis that the increase in sediment concentration is related to temporary channel and riverbank erosion. The clockwise hysteresis loops observed in this study are consistent with findings by Favaro and Lamoureux (2014), who observe varying hysteresis patterns in the High Arctic depending on sediment availability. The sediment concentration is much lower in the summer of 2016, which implies, that all the available sediment has been flushed out of the system during the snowmelt period of 2016. Thus, the summer of 2016 did not seem to be influenced by the event anymore. This short-lived sediment mobilization differs from major disturbances such as active-layer detachments or retrogressive thaw slumps, which impact sediment delivery in streams over many seasons (Bowden et al. 2008; Frey and McClelland 2009; Lamoureux and Lafrenière 2009; Kokelj et al. 2013; Lamoureux and Lafrenière 2017). Along with the increased sediment flux in 2015, we observe higher chloride concentrations and a slightly reduced alkalinity compared with the other years. The declining calcium carbonate source could indicate erosion of marine sediments, found on Herschel Island (Fritz et al. 2012). High TDS concentrations are known to correspond to groundwater contribution and may increase across the Arctic in the future (Frey and McClelland 2009). We find varying concentrations over the 3 years of monitoring. The concentration minima in 2015 could point towards greater surface water and less ground water contribution than in the other years.

We compare our SS flux estimates for 2015 and 2016 to other Arctic locations scaled to 17-day periods (Table 4) and find that our very low 2016 estimate is comparable to measurements at Boothia Peninsula in the High Arctic ( $100\text{--}300 \text{ kg km}^{-2}$ ). Our high 2015 estimate exceeds values from Melville Island in the High Arctic ( $3200\text{--}6300 \text{ kg km}^{-2}$ ) and also the Lena River ( $2300 \text{ kg km}^{-2}$ ), but remains below fluxes from the Mackenzie River ( $20\ 300 \text{ kg km}^{-2}$ ) and the disturbed Slump D nearby on Herschel Island ( $2.4 \times 10^6 \text{ kg km}^{-2}$ ). Transport of suspended sediment is highly variable across the Arctic region, and especially at our site, and between years. We do not find an increase of suspended sediment yield with decreasing watershed size as proposed by Walling (1983) or Fryirs (2013) although this may be due to the fact that the values compiled here are covering a range of latitudes, geological settings and ecoregions, thus influencing this relationship. We also do not have other sites in the Low Arctic to compare our estimates to. Monitoring of small watersheds over several years is essential to capture interannual dynamics and to establish reliable flux estimates. The high 2015 estimate is similar to the sum of the six large Arctic Rivers ( $8470 \text{ kg km}^{-2}$ ) underlining the importance of extended monitoring.

We find that 2.0% of the suspended sediment is composed of POC in our study site. This finding corresponds to the study at Cape Bounty in the High Canadian Arctic by Lamoureux and Lafrenière (2014), who also find a linear relationship between POC and SSC (Table 4). There, East River with an area of  $11.6 \text{ km}^2$  shows a POC/SSC ratio of 2.2%, whereas West River ( $8.0 \text{ km}^2$ ) shows a ratio of 2.0%. Also, ratios of the Ob and Mackenzie rivers (Holmes et al. 2002; Carrizo and Gustafsson 2011) are in a similar range as our study site. The melt-water stream draining Slump D nearby our study site has a mean POC to SSC ratio of 1.7% for the summer monitoring periods. The ratio is the same for the large Arctic Rivers (without Yukon River). Contrary to the studies where annual fluxes are reported, our estimates are only based on the periods of stream monitoring in the summer. The POC to SSC ratio is unknown during snowmelt at our study site.

Local geomorphology may influence fluxes of DOC, TDS, and SS to the ocean. The Ice Creek watershed flows through an alluvial fan before draining into the Beaufort Sea, which is why we collected water samples along the fan outflows to investigate how concentrations

**Table 4.** Sediment and particulate organic carbon (POC) yield values for various Arctic locations sorted by 17-day suspended sediment (SS) yields.

| Catchment                  | Study   | Area                       | Size (km <sup>2</sup> ) | 17-day SS yield (kg km <sup>-2</sup> ) | SS Yield (kg yr <sup>-1</sup> km <sup>-2</sup> ) | POC yield (kg yr <sup>-1</sup> km <sup>-2</sup> ) | POC:SS (conc.) (%) | POC:SS (yields) (%) |
|----------------------------|---|----------------------------|-------------------------|--|--|---|--------------------|---------------------|
| West Tributary             | Forbes and Lamoureux 2005                       | Boothia Peninsula, Nunavut | 345                     | 100                                    | 200  | NA  | NA                 | NA                  |
| East Tributary             | Forbes and Lamoureux 2005                       | Boothia Peninsula, Nunavut | 465                     | 300                                    | 1250   | NA  | NA                 | NA                  |
| Lord Lindsey River         | Forbes and Lamoureux 2005                       | Boothia Peninsula, Nunavut | 1485                    | 300                                    | 1150   | NA  | NA                 | NA                  |
| Ice Creek West 2016        | This Study <sup>a</sup>                         | Yukon Coast                | 1.4                     | 360                                    | NA   | NA  | 2.0                | NA                  |
| Yenisei                    | Holmes et al. 2002; Carrizo and Gustafsson 2011 | West Siberian Lowlands     | 2.4 × 10 <sup>6</sup>   | 500                                    | 1900   | 70  | NA                 | 3.7                 |
| Lena                       | Holmes et al. 2002; Carrizo and Gustafsson 2011 | Central Siberian Plateau   | 2.43 × 10 <sup>6</sup>  | 2300                                   | 8500   | 240   | NA                 | 2.8                 |
| East River                 | Lamoureux and Lafrenière 2014                   | Melville Island, Nunavut   | 11.6                    | 3200                                   | 11 500   | 90  | 2.2                | 0.8                 |
| Kolyma                     | Holmes et al. 2002; Carrizo and Gustafsson 2011 | East Siberian Highlands    | 5.3 × 10 <sup>5</sup>   | 5200                                   | 19 000   | 490   | NA                 | 2.6                 |
| West River                 | Lamoureux and Lafrenière 2014                   | Melville Island, Nunavut   | 8                       | 6300                                   | 23 000   | 270   | 2.0                | 1.2                 |
| Anaktuvuk                  | Lamb and Toniolo 2016                           | Alaska North Slope         | 7000                    | 6600                                   | 24 000   | NA  | NA                 | NA                  |
| Ice Creek West 2015        | This Study <sup>a</sup>                         | Yukon Coast                | 1.4                     | 7245                                   | NA   | NA  | NA                 | NA                  |
| Yukon                      | Chikita et al. 2012                             | Yukon                      | 8.3 × 10 <sup>5</sup>   | 15 500                                 | 56 630   | 590   | NA                 | 0                   |
| Chandler                   | Lamb and Toniolo 2016                           | Alaska North Slope         | 5800                    | 19 000                                 | 69 350   | NA  | NA                 | NA                  |
| Mackenzie                  | Holmes et al. 2002; Carrizo and Gustafsson 2011 | North American Cordillera  | 1.68 × 10 <sup>6</sup>  | 20 300                                 | 74 000   | 1250  | NA                 | 1.7                 |
| Itkillit                   | Lamb and Toniolo 2016                           | Alaska North Slope         | 1900                    | 21 300                                 | 77 720   | NA  | NA                 | NA                  |
| Slump D                    | Weege 2016                                      | Yukon Coast                | 0.136                   | 2.4 × 10 <sup>6</sup>                  | NA   | 40 600 <sup>b</sup>                               | NA                 | 1.7                 |
| Arctic Rivers <sup>c</sup> | Holmes et al. 2002                              | Circum-Arctic              | 1.09 × 10 <sup>7</sup>  | 8470                                   | 181 800  | 320   | NA                 | 1.7                 |

**Note:** Numbers from the literature were reduced to significant digits. NA, not available.

<sup>a</sup>Due to the high variability between both 2015 and 2016, no mean was calculated, but seasons were included separately.

<sup>b</sup>The mean POC yield for Slump D only accounts for 17 days of monitoring in 2011 and 2012.

<sup>c</sup>The POC to suspended sediment concentration (SSC) ratio was calculated based on the total POC and SSC for all five large Arctic Rivers. The value does not include the Yukon River.

might have been modified (Table 2). Sediment concentration is highly variable whereas DOC and TDS are similar to the output from the Ice Creek watersheds. Since it was not possible to measure the discharge of the fan outlets, we cannot give any estimate on how the overall flux was altered. This issue should be addressed in future studies.

#### Rainfall response and flow pathways

The strong positive relationship between runoff and DOC flux, and the anti-clockwise hysteretic pattern of the individual rainfall events suggest that DOC is widely available throughout the catchment. Highest DOC concentrations typically occur on the falling hydrograph. This finding is consistent to discharge–DOC hysteresis patterns in subarctic Alaska (Petronne et al. 2007).

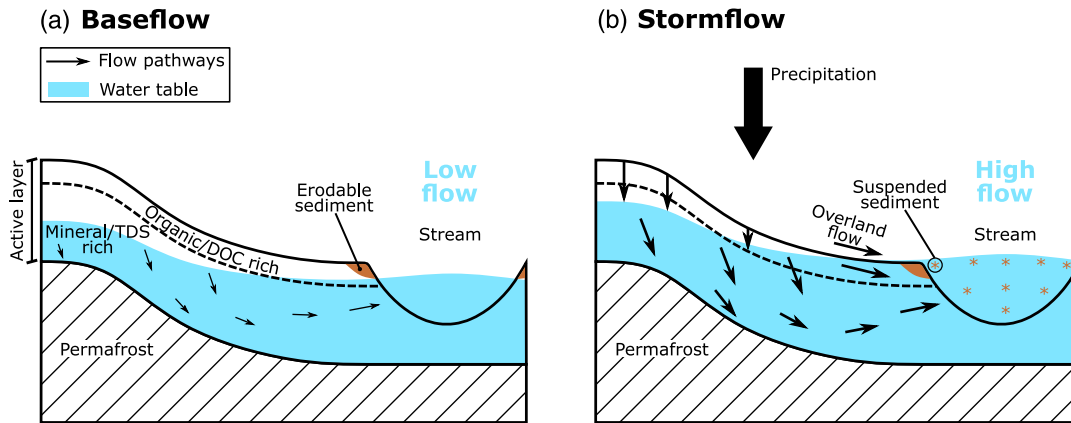
Contrary behaviour is observed at another subarctic, alpine location, where a clockwise hysteresis is visible indicating a finite source of DOC in the watershed (Carey 2003). Highest DOC concentrations occur on the ascending hydrograph and decline rapidly after. The authors assume that DOC is flushed of organic soils followed by a decline of concentrations during later storm events in the season. This decline there may be explained by a declining contributing source, deeper flow pathways as the season progresses and exhaustion of soluble organic carbon due to flushing from previous storm events. For our watershed on Herschel Island, we could not detect any limitation of DOC. This suggests that DOC is widely available and sourced from near-surface pathways.

Contrasting to the DOC behaviour, we observe clockwise hysteretic patterns between discharge and TDS during rain events, which suggest a limitation of TDS in the catchment. Highest concentrations are found on the ascending hydrograph, and peak values decrease as the season progresses. Based on this, we assume that the TDS sources are present deeper in the active layer, and predominantly accessed during low flow conditions. As rainfall occurs and water level rises, major ions are diluted. The change of flow pathways further may impede the access to the TDS source.

Suspended sediment in our catchment is mobilized rapidly with the onset of rain until a threshold is reached, declining rapidly thereafter despite of high remaining flows. The timing of SSC and discharge peaks is variable in our study site. Both initiating rainfall events (2015-1 and 2016-1) show peak SSC after peak discharge occurred (anti-clockwise hysteresis), although some uncertainty exists regarding 2016-1 due to the late onset of SSC monitoring and the lower frequency of sampling. Based on the discharge–SSC behaviour for the remaining 2016 events, we assume that the recorded SSC peak concentration was the actual peak concentration of the entire event. Runoff and channelization need to progress to access the sediments. The subsequent events in both seasons show a predominantly clockwise hysteresis pattern, whereas the 2015 SSC peaks occur at peak flow, and the 2016 SSC peaks before peak flow. This contrasting behaviour highlights the difference in sediment mobilization when comparing both seasons. While channelization progress and runoff increase were very important in 2015, sediment was accessed already during lower flows in 2016. Discharge suspended sediment hysteresis is observed at other sites during the nival period showing both, clockwise and anti-clockwise patterns (Chikita et al. 2012; Favaro and Lamoureux 2015). During rainfall, the observed behaviour is predominantly clockwise (Braun et al. 2000; Forbes and Lamoureux 2005). The limitation of sediment supply has also been described in other Arctic locations by Cogley and McCann (1976) and Woo and Sauriol (1981).

Based on hysteresis analysis of the different hydrochemical parameters, a conceptual model of flow pathways and water quality is presented in Figure 9. At baseflow or low flow conditions water is routed deeper in the active layer through the mineral soil leaching little DOC and more TDS. With the onset of rain, organic-rich pathways at or near the surface are

**Fig. 9.** Conceptual model of rainfall response in Ice Creek West showing the difference between (a) baseflow and (b) stormflow conditions. The water table is indicated in blue. The upper part of the active layer is organic rich and the source of DOC, whereas the mineral rich deeper part of the active layer is the source of TDS. Sediment (brown) that is mobilized as suspended sediment during stormflow is located near the river channel.



accessed delivering high amounts of DOC, and, at the same time, diluting baseflow water. TDS may recover during baseflow conditions and with deepening of the active layer as the season progresses. This model shares many similarities to [Quinton and Marsh \(1999\)](#), and beyond that, it links runoff processes and water quality.

Hydrochemical sampling along transects of the outflow channel may help to understand whether the measured water quality of the outflow reflects conditions of the entire watershed. This would help to constrain local sources of sediment, TDS, and organic matter, and to gain more insights into lateral matter transport.

## Conclusions

This study investigates hydrology and water quality of a coastal watershed in a Low Arctic setting with regard to summer rainfall impacts. We find that the Ice Creek West watershed is characterized by a nival flow regime with snowmelt being the largest hydrological event of the year. The catchment responds quickly to hydrological inputs reflecting the relatively small catchment size. Summer rainfall events of different magnitudes are observed during the summers 2014–2016. Flow during the summer is strongly dependent on the input of rain, and thus, also controls water quality and fluxes.

TDS and sediment supply are limited in the catchment as indicated by clockwise hysteresis patterns. We further find a strong interannual variability of both parameters, depending on local sediment sources and erosion processes. Approximately 2.0% of suspended sediment is composed of POC. The conceptual model of flow pathways suggests that, during baseflow conditions, water is routed through the subsurface accessing solutes from the mineral soil deeper in the active layer. During rainfall, shallower near-surface pathways are activated, which deliver organic rich material, which is then exported out of the catchment. It appears that DOC is widely available throughout the watershed, and that its flux proportionally increases with total runoff. We also found a proportionate increase of TDS flux with runoff. This has implications for anticipated increasing summer rainfall in the Arctic, which would likely lead to an increase of DOC and TDS fluxes from the catchment.

Future studies should extend the monitoring to fully understand the interannual variability of sediment transport, to establish a baseline. Capturing the snowmelt period is

essential to determine the hydrochemical fluxes during this largest hydrological event of the year. Sampling along the stream would help to understand how concentrations are modified downstream, and where DOC, TDS, and SS sources are located. This would contribute to an understanding how landcover, soil types, and disturbances influence the overall flux from a watershed. Ultimately, results from this Low Arctic site could contribute to upscaling efforts of DOC, TDS, and SS flux to the Arctic Ocean.

### Data availability

Data have been made available through PANGAEA and can be accessed following the link: <https://doi.pangaea.de/10.1594/PANGAEA.888180>.

### Author contribution

Hugues Lantuit, Scott Lamoureux, and Caroline Coch developed the study design. Field work was conducted by Jaroslav Obu in 2014, by Isabell Eischeid in 2015, and by Caroline Coch in 2016. Christian Knoblauch ran lab analyzes for POC, DOC, and TDN of 2015–2016 samples. Michael Fritz performed lab analyzes of the 2014 samples. Caroline Coch ran lab analyzes, processed all data, and prepared the manuscript with contributions from all co-authors.

### Competing interests

The authors declare that they have no conflict of interest.

### Acknowledgements

We are grateful to the Yukon Territorial Government, Yukon Parks (Herschel Island Qikiqtaruk Territorial Park), and the Aurora Research Institute for their support during this project. This work was funded by the Helmholtz Association (grant no. VH-NG-801 to Hugues Lantuit), and it has received funding under the European Union's Horizon 2020 research and innovation programme under grant agreement No. 773421. C. Coch received a scholarship from the Studienstiftung des deutschen Volkes.

The authors wish to thank Antje Eulenburg, Birgit Grabellus, Marek Jaskólski, Jan Kahl, Ute Kuschel, Nicole Mätzing, Paul Overduin, Saskia Ruttor, Julian Schneider, Samuel Stettner, and George Tanski for their help in the instrumentation set up, data collection in the field, and laboratory analyzes. A special thanks to Cameron Eckert, Richard Gordon, Ricky Joe, Paden Lennie, Edward McLeod, and Samuel McLeod for their support and helpful insights in the field. Thank you to Juan Estrella-Martínez for help with the schematic and statistical analyzes.

### References

- Bintanja, R., and Andry, O. 2017. Towards a rain-dominated Arctic. *Nat. Clim. Change*, **7**: 263–267. doi: [10.1038/nclimate3240](https://doi.org/10.1038/nclimate3240).
- Bowden, W.B., Gooseff, M.N., Balsler, A., Green, A., Peterson, B.J., and Bradford, J. 2008. Sediment and nutrient delivery from thermokarst features in the foothills of the North Slope, Alaska: potential impacts on headwater stream ecosystems. *J. Geophys. Res.: Biogeosci.* **113**: G02026. doi: [10.1029/2007jg000470](https://doi.org/10.1029/2007jg000470).
- Braun, C., Hardy, D.R., Bradley, R.S., and Retelle, M.J. 2000. Streamflow and suspended sediment transfer to Lake Sophia, Cornwallis Island, Nunavut, Canada. *Arct. Antarct. Alp. Res.* **32**: 456–465. doi: [10.1080/15230430.2000.12003390](https://doi.org/10.1080/15230430.2000.12003390).
- Burn, C.R. 2012. *Herschel Island Qikiqtaryuk: a natural and cultural history of Yukon's Arctic Island*. University of Calgary Press, Calgary, Alta., Canada.
- Burn, C.R., and Zhang, Y. 2009. Permafrost and climate change at Herschel Island (Qikiqtaruq), Yukon Territory, Canada. *J. Geophys. Res.: Earth Surf.* **114**: F02001. doi: [10.1029/2008JF001087](https://doi.org/10.1029/2008JF001087).
- Carey, S.K. 2003. Dissolved organic carbon fluxes in a discontinuous permafrost subarctic alpine catchment. *Permafr. Periglac. Processes*, **14**: 161–171. doi: [10.1002/ppp.444](https://doi.org/10.1002/ppp.444).

- Carey, S.K., Boucher, J.L., and Duarte, C.M. 2013. Inferring groundwater contributions and pathways to streamflow during snowmelt over multiple years in a discontinuous permafrost subarctic environment (Yukon, Canada). *Hydrogeol. J.* **21**: 67–77. doi: [10.1007/s10040-012-0920-9](https://doi.org/10.1007/s10040-012-0920-9).
- Carrizo, D., and Gustafsson, O. 2011. Pan-arctic river fluxes of polychlorinated biphenyls. *Environ. Sci. Technol.* **45**: 8377–8384. doi: [10.1021/es201766z](https://doi.org/10.1021/es201766z). PMID: 21863827.
- CAVM Team. 2003. Circumpolar Arctic Vegetation Map (1:7 500 000 scale). Conservation of Arctic Flora and Fauna (CAFF) Map No. 1. U.S. Fish and Wildlife Service, Anchorage, Alaska, USA.
- Chikita, K.A., Wada, T., Kudo, I., and Kim, Y. 2012. The intra-annual variability of discharge, sediment load and chemical flux from the monitoring: the Yukon River, Alaska. *J. Water Resour. Prot.* **04**: 173–179. doi: [10.4236/jwarp.2012.44020](https://doi.org/10.4236/jwarp.2012.44020).
- Cockburn, J.M.H., and Lamoureux, S.F. 2008. Hydroclimate controls over seasonal sediment yield in two adjacent High Arctic watersheds. *Hydrol. Processes*, **22**: 2013–2027. doi: [10.1002/hyp.6798](https://doi.org/10.1002/hyp.6798).
- Cogley, J.G., and McCann, S.B. 1976. An exceptional storm and its effects in the Canadian High Arctic. *Arct. Alp. Res.* **8**: 105. doi: [10.2307/1550613](https://doi.org/10.2307/1550613).
- Dedkov, A. 2004. The relationship between sediment yield and drainage basin area. Pages 197–204 in V. Golosov, V. Belyaev, and D.E. Walling, eds. *Sediment transfer through the fluvial system*. IAHS, Moscow, Russia.
- Dugan, H.A., Lamoureux, S.F., Lafrenière, M.J., and Lewis, T. 2009. Hydrological and sediment yield response to summer rainfall in a small high Arctic watershed. *Hydrol. Processes*, **23**: 1514–1526. doi: [10.1002/hyp.7285](https://doi.org/10.1002/hyp.7285).
- Dugan, H.A., Lamoureux, S.F., Lewis, T., and Lafrenière, M.J. 2012. The impact of permafrost disturbances and sediment loading on the limnological characteristics of two high Arctic lakes. *Permafrost. Periglac. Processes*, **23**: 119–126. doi: [10.1002/ppp.1735](https://doi.org/10.1002/ppp.1735).
- Environment and Climate Change Canada. 2018. Historical Data. Environment and Climate Change Canada. [Online]. Available from [http://climate.weather.gc.ca/historical\\_data/search\\_historic\\_data\\_e.html](http://climate.weather.gc.ca/historical_data/search_historic_data_e.html) [05 Apr. 2018].
- Favaro, E.A., and Lamoureux, S.F. 2014. Antecedent controls on rainfall runoff response and sediment transport in a high Arctic catchment. *Geogr. Ann. Ser. A Phys. Geogr.* **96**: 433–446. doi: [10.1111/geoa.12063](https://doi.org/10.1111/geoa.12063).
- Favaro, E.A., and Lamoureux, S.F. 2015. Downstream patterns of suspended sediment transport in a High Arctic river influenced by permafrost disturbance and recent climate change. *Geomorphology*, **246**: 359–369. doi: [10.1016/j.geomorph.2015.06.038](https://doi.org/10.1016/j.geomorph.2015.06.038).
- Forbes, A.C., and Lamoureux, S.F. 2005. Climatic controls on streamflow and suspended sediment transport in three large middle Arctic catchments, Boothia Peninsula, Nunavut, Canada. *Arct. Antarct. Alp. Res.* **37**: 304–315. doi: [10.1657/1523-0430\(2005\)037\[0304:CCOSAS\]2.0.CO;2](https://doi.org/10.1657/1523-0430(2005)037[0304:CCOSAS]2.0.CO;2).
- Fouché, J., Lafrenière, M.J., Rutherford, K., and Lamoureux, S. 2017. Seasonal hydrology and permafrost disturbance impacts on dissolved organic matter composition in High Arctic headwater catchments. *Arct. Sci.* **3**: 378–405. doi: [10.1139/as-2016-0031](https://doi.org/10.1139/as-2016-0031).
- Freeze, R.A., and Cherry, J.A. 1979. *Groundwater*. Prentice-Hall, Englewood Cliffs, N.J., USA.
- Frey, K.E., and McClelland, J.W. 2009. Impacts of permafrost degradation on arctic river biogeochemistry. *Hydrol. Processes*, **23**: 169–182. doi: [10.1002/hyp.7196](https://doi.org/10.1002/hyp.7196).
- Fritz, M., Wetterich, S., Schirrmeister, L., Meyer, H., Lantuit, H., Preusser, F., and Pollard, W.H. 2012. Eastern Beringia and beyond: late Wisconsinan and Holocene landscape dynamics along the Yukon Coastal Plain, Canada. *Palaeogeogr., Palaeoclimatol., Palaeoecol.* **319–320**: 28–45. doi: [10.1016/j.palaeo.2011.12.015](https://doi.org/10.1016/j.palaeo.2011.12.015).
- Fritz, M., Opel, T., Tanski, G., Herzsuh, U., Meyer, H., Eulenburg, A., and Lantuit, H. 2015. Dissolved organic carbon (DOC) in Arctic ground ice. *The Cryosphere*, **9**: 737–752. doi: [10.5194/tc-9-737-2015](https://doi.org/10.5194/tc-9-737-2015).
- Fryirs, K. 2013. (Dis)Connectivity in catchment sediment cascades: a fresh look at the sediment delivery problem. *Earth Surf. Processes Landforms*, **38**: 30–46. doi: [10.1002/esp.3242](https://doi.org/10.1002/esp.3242).
- Gordeev, V.V. 2006. Fluvial sediment flux to the Arctic Ocean. *Geomorphology*, **80**: 94–104. doi: [10.1016/j.geomorph.2005.09.008](https://doi.org/10.1016/j.geomorph.2005.09.008).
- Holmes, R.M., McClelland, J.W., Peterson, B.J., Shiklomanov, I.A., Shiklomanov, A.I., Zhulidov, A.V., Gordeev, V.V., and Bobrovitskaya, N.N. 2002. A circumpolar perspective on fluvial sediment flux to the Arctic Ocean. *Global Biogeochem. Cycles*, **16**: 451–4514. doi: [10.1029/2001GB001849](https://doi.org/10.1029/2001GB001849).
- Holmes, R.M., McClelland, J.W., Peterson, B.J., Tank, S.E., Bulygina, E., Eglinton, T.I., Gordeev, V.V., Gurtovaya, T.Y., Raymond, P.A., Repeta, D.J., Staples, R., Striegl, R.G., Zhulidov, A.V., and Zimov, S.A. 2012. Seasonal and annual fluxes of nutrients and organic matter from large rivers to the Arctic Ocean and surrounding seas. *Estuaries Coasts*, **35**: 369–382. doi: [10.1007/s12237-011-9386-6](https://doi.org/10.1007/s12237-011-9386-6).
- Klein, M. 1984. Anti clockwise hysteresis in suspended sediment concentration during individual storms: Holbeck catchment; Yorkshire, England. *Catena*, **11**: 251–257. doi: [10.1016/0341-8162\(84\)90014-6](https://doi.org/10.1016/0341-8162(84)90014-6).
- Kokelj, S.V., Lacelle, D., Lantz, T.C., Tunnicliffe, J., Malone, L., Clark, I.D., and Chin, K.S. 2013. Thawing of massive ground ice in mega slumps drives increases in stream sediment and solute flux across a range of watershed scales. *J. Geophys. Res. Earth Surf.* **118**: 681–692. doi: [10.1002/jgrf.20063](https://doi.org/10.1002/jgrf.20063).
- Lamb, E., and Toniolo, H. 2016. Initial quantification of suspended sediment loads for three Alaska north slope rivers. *Water*, **8**: 419. doi: [10.3390/w8100419](https://doi.org/10.3390/w8100419).
- Lamoureux, S.F., and Lafrenière, M.J. 2009. Fluvial Impact of extensive active layer detachments, Cape Bounty, Melville Island, Canada. *Arct. Antarct. Alp. Res.* **41**: 59–68. doi: [10.1657/1523-0430-41.1.59](https://doi.org/10.1657/1523-0430-41.1.59).
- Lamoureux, S.F., and Lafrenière, M.J. 2014. Seasonal fluxes and age of particulate organic carbon exported from Arctic catchments impacted by localized permafrost slope disturbances. *Environ. Res. Lett.* **9**: 045002. doi: [10.1088/1748-9326/9/4/045002](https://doi.org/10.1088/1748-9326/9/4/045002).

- Lamoureux, S.F., and Lafrenière, M.J. 2017. More than just snowmelt: integrated watershed science for changing climate and permafrost at the Cape Bounty Arctic Watershed Observatory. *WIREs Water*, **5**: e1255. doi: [10.1002/wat2.1255](https://doi.org/10.1002/wat2.1255).
- Lantuit, H., and Pollard, W.H. 2008. Fifty years of coastal erosion and retrogressive thaw slump activity on Herschel Island, southern Beaufort Sea, Yukon Territory, Canada. *Geomorphology*, **95**: 84–102. doi: [10.1016/j.geomorph.2006.07.040](https://doi.org/10.1016/j.geomorph.2006.07.040).
- Laudon, H., Köhler, S., and Buffam, I. 2004. Seasonal TOC export from seven boreal catchments in northern Sweden. *Aquat. Sci.* **66**: 223–230. doi: [10.1007/s00027-004-0700-2](https://doi.org/10.1007/s00027-004-0700-2).
- Lewis, T., Braun, C., Hardy, D.R., Francus, P., and Bradley, R.S. 2005. An extreme sediment transfer event in a Canadian High Arctic stream. *Arct. Antarct. Alp. Res.* **37**: 477–482. doi: [10.1657/1523-0430\(2005\)037\[0477:AESTEJ\]2.0.CO;2](https://doi.org/10.1657/1523-0430(2005)037[0477:AESTEJ]2.0.CO;2).
- Mackay, J.R. 1959. Glacier ice-thrust features of the Yukon Coast. *Geogr. Bull.* **13**: 5–21.
- MacLean, R., Oswood, M.W., Irons, J.G., III., and McDowell, W.H. 1999. The effect of permafrost on stream biogeochemistry: a case study of two streams in the Alaskan (U.S.A.) taiga. *Biogeochemistry*, **47**: 239–267. doi: [10.1007/BF00992909](https://doi.org/10.1007/BF00992909).
- Myers-Smith, I.H., Forbes, B.C., Wilmking, M., Hallinger, M., Lantz, T., Blok, D., Tape, K.D., Macias-Fauria, M., Sass-Klaassen, U., Lévesque, E., Boudreau, S., Ropars, P., Hermanutz, L., Trant, A., Collier, L.S., Weijers, S., Rozema, J., Rayback, S.A., Schmidt, N.M., Schaepman-Strub, G., Wipf, S., Rixen, C., Ménard, C.B., Venn, S., Goetz, S., Andreu-Hayles, L., Elmendorf, S., Ravolainen, V., Welker, J., Grogan, P., Epstein, H.E., and Hik, D.S. 2011. Shrub expansion in tundra ecosystems: dynamics, impacts and research priorities. *Environ. Res. Lett.* **6**: 045509. doi: [10.1088/1748-9326/6/4/045509](https://doi.org/10.1088/1748-9326/6/4/045509).
- Obu, J., Lantuit, H., Myers-Smith, I., Heim, B., Wolter, J., and Fritz, M. 2017. Effect of terrain characteristics on soil organic carbon and total nitrogen stocks in soils of Herschel Island, western Canadian Arctic. *Permafr. Periglac. Processes*, **28**: 92–107. doi: [10.1002/ppp.1881](https://doi.org/10.1002/ppp.1881).
- Peterson, B.J., Holmes, R.M., McClelland, J.W., Vorosmarty, C.J., Lammers, R.B., Shiklomanov, A.I., Shiklomanov, I.A., and Rahmstorf, S. 2002. Increasing river discharge to the Arctic Ocean. *Science*, **298**: 2171–2173. doi: [10.1126/science.1077445](https://doi.org/10.1126/science.1077445). PMID: 12481132.
- Petrone, K.C., Jones, J.B., Hinzman, L.D., and Boone, R.D. 2006. Seasonal export of carbon, nitrogen, and major solutes from Alaskan catchments with discontinuous permafrost. *J. Geophys. Res.* **111**: G02020. doi: [10.1029/2006JG000281](https://doi.org/10.1029/2006JG000281).
- Petrone, K.C., Hinzman, L.D., Shibata, H., Jones, J.B., and Boone, R.D. 2007. The influence of fire and permafrost on sub-arctic stream chemistry during storms. *Hydrol. Processes*, **21**: 423–434. doi: [10.1002/hyp.6247](https://doi.org/10.1002/hyp.6247).
- Pollard, W.H. 1990. The nature and origin of ground ice in the Herschel Island area, Yukon Territory. *Proc. Fifth Canadian Conference on Permafrost, Québec, Que., Canada*. pp. 23–30.
- Quinton, W.L., and Marsh, P. 1999. A conceptual framework for runoff generation in a permafrost environment. *Hydrol. Processes*, **13**: 2563–2581. doi: [10.1002/\(SICI\)1099-1085\(199911\)13:16<2563::AID-HYP942>3.0.CO;2-D](https://doi.org/10.1002/(SICI)1099-1085(199911)13:16<2563::AID-HYP942>3.0.CO;2-D).
- Radosavljevic, B., Lantuit, H., Pollard, W., Overduin, P., Couture, N., Sachs, T., Helm, V., and Fritz, M. 2015. Erosion and flooding — threats to coastal infrastructure in the Arctic: a case study from Herschel Island, Yukon Territory, Canada. *Estuaries Coasts*, **39**: 900–915. doi: [10.1007/s12237-015-0046-0](https://doi.org/10.1007/s12237-015-0046-0).
- Rampton, V.N. 1982. Quaternary geology of the Yukon Coastal Plain. Geological Survey of Canada, Ottawa, Ont., Canada.
- Semkin, R.G., Mierle, G., and Neureuther, R.J. 2005. Hydrochemistry and mercury cycling in a High Arctic watershed. *Sci. Total Environ.* **342**: 199–221. doi: [10.1016/j.scitotenv.2004.12.047](https://doi.org/10.1016/j.scitotenv.2004.12.047). PMID: 15866276.
- Singh, V. 1992. Elementary hydrology. Prentice Hall, Englewood Cliffs, N.J., USA.
- Skogerboe, G.V., Walker, W.R., and Bennett, R.S. 1973. Generalized discharge relations for cutthroat flumes. *J. Irrig. Drain Div.* **98**: 569–583. doi: [10.13031/2013.37449](https://doi.org/10.13031/2013.37449).
- Smith, C.A.S., Kennedy, C.E., Hargrave, A.E., and McKenna, K.M. 1989. Soil and vegetation of Herschel island, Yukon Territory. Land Resource Research Centre, Agriculture Canada, Ottawa, Ont., Canada.
- Spence, C., Kokelj, S.V., Kokelj, S.A., McCluskie, M., and Hedstrom, N. 2015. Evidence of a change in water chemistry in Canada's subarctic associated with enhanced winter streamflow. *J. Geophys. Res.: Biogeosci.* **120**: 113–127. doi: [10.1002/2014JG002809](https://doi.org/10.1002/2014JG002809).
- Tank, S.E., Fellman, J.B., Hood, E., and Kritzberg, E.S. 2018. Beyond respiration: controls on lateral carbon fluxes across the terrestrial-aquatic interface. *Limnol. Oceanogr. Lett.* **3**: 76–88. doi: [10.1002/lol2.10065](https://doi.org/10.1002/lol2.10065).
- Tanski, G., Couture, N., Lantuit, H., Eulenburg, A., and Fritz, M. 2016. Eroding permafrost coasts release low amounts of dissolved organic carbon (DOC) from ground ice into the nearshore zone of the Arctic Ocean. *Global Biogeochem. Cycles*, **30**: 1054–1068. doi: [10.1002/2015GB005337](https://doi.org/10.1002/2015GB005337).
- Vonk, J.E., Tank, S.E., Bowden, W.B., Laurion, I., Vincent, W.F., Alekseychik, P., Amyot, M., Billet, M.F., Canário, J., Cory, R.M., Deshpande, B.N., Helbig, M., Jammet, M., Karlsson, J., Larouche, J., MacMillan, G., Rautio, M., Walter Anthony, K.M., and Wickland, K.P. 2015. Reviews and syntheses: effects of permafrost thaw on Arctic aquatic ecosystems. *Biogeosciences*, **12**: 7129–7167. doi: [10.5194/bg-12-7129-2015](https://doi.org/10.5194/bg-12-7129-2015).
- Walling, D.E. 1983. The sediment delivery problem. *J. Hydrol.* **65**: 209–237. doi: [10.1016/0022-1694\(83\)90217-2](https://doi.org/10.1016/0022-1694(83)90217-2).
- Weege, S. 2016. Climatic drivers of retrogressive thaw slump activity and resulting sediment and carbon release to the nearshore zone of Herschel Island, Yukon Territory, Canada. Ph.D. thesis, Universität Potsdam, Potsdam. Mathematisch-Naturwissenschaftliche Fakultät/Institut für Erd- und Umweltwissenschaften.
- Wegner, C., Bennett, K.E., de Vernal, A., Forwick, M., Fritz, M., Heikkilä, M., Łącka, M., Lantuit, H., Laska, M., Moskalik, M., O'Regan, M., Pawłowska, J., Promińska, A., Rachold, V., Vonk, J.E., and Werner, K. 2015.

Variability in transport of terrigenous material on the shelves and the deep Arctic Ocean during the Holocene. *Polar Res.* **34**: 24964. doi: [10.3402/polar.v34.24964](https://doi.org/10.3402/polar.v34.24964).  
 Woo, M. 2012. Permafrost hydrology. Springer, Heidelberg, Germany.  
 Woo, M., and Sauriol, J. 1981. Effects of snow jams on fluvial activities in the High Arctic. *Phys. Geogr.* **2**: 83–98. doi: [10.1080/02723646.1981.10642206](https://doi.org/10.1080/02723646.1981.10642206).

## Appendix A

**Fig. A1.** Comparison of rainfall data obtained from the Environment Canada station and the weather station deployed in Ice Creek West between 15 June and 3 Aug. 2016. The ribbon around the regression line indicates the standard error. The dominant wind direction [northwest (NW) or south-southeast (SSE)] is colour-coded for each point. Wind direction is reported as not available when the maximum gust is below  $31 \text{ km h}^{-1}$ . This was the case for 12 data points ([Environment and Climate Change Canada 2018](#)).

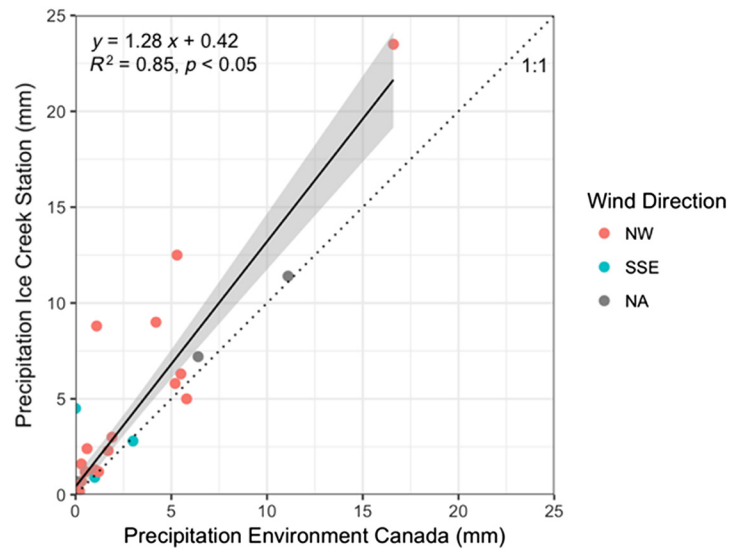


**Fig. A2.** Differences in sample treatment. DOC concentrations of samples that were directly treated in the field (unfrozen) are plotted against those of samples that were frozen in the field and treated later on in the laboratory (frozen). The ribbon around the regression line indicates the standard error.

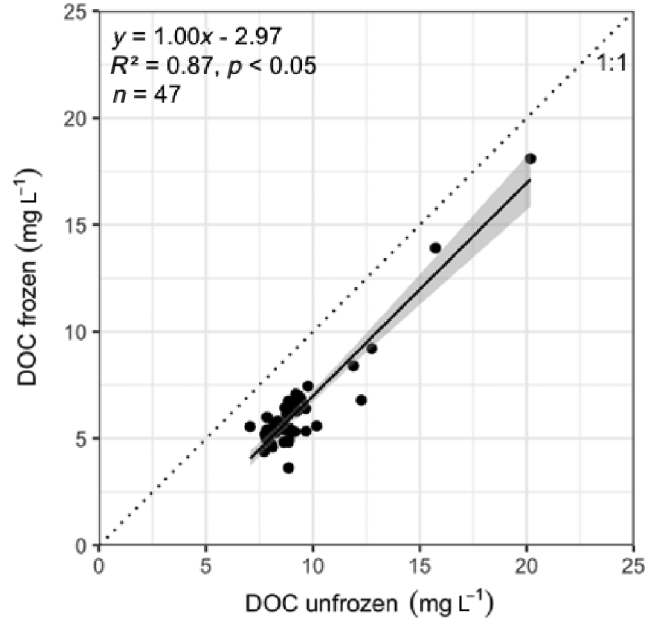


**Fig. A3.** Hydrological year of 2015/2016 showing (a) precipitation (mm) and temperature (°C), (b) recorded runoff (m<sup>3</sup> s<sup>-1</sup>) in the catchment, (c) conductivity, and (d) diel curves of mean discharged averaged over Julian weeks 21 until 28.

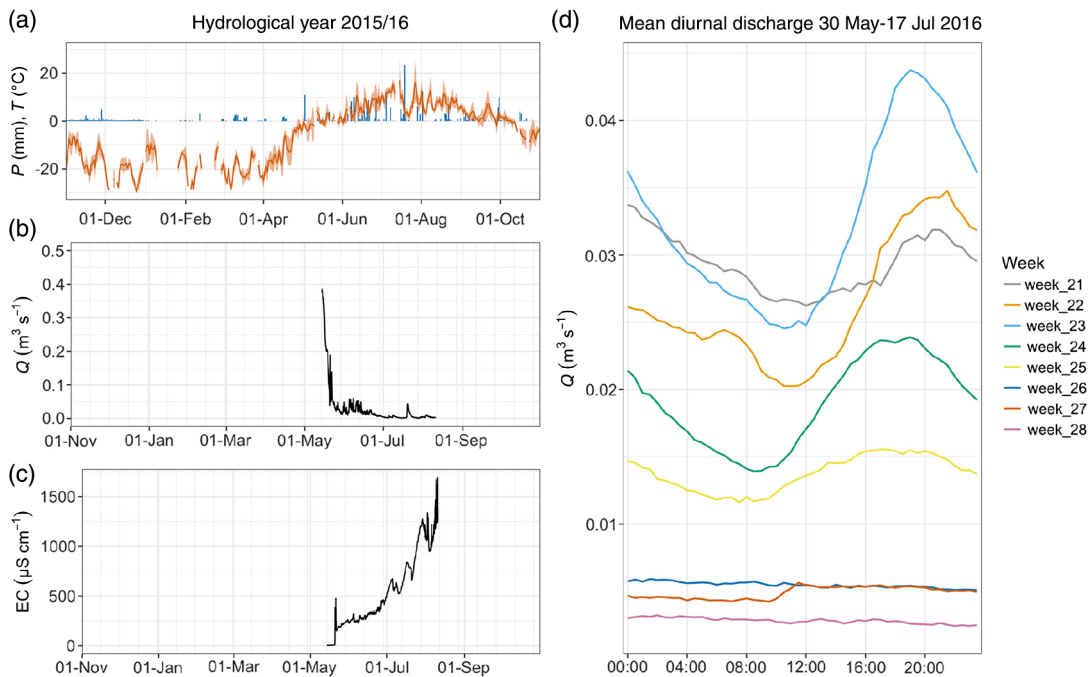


**Fig. A4.** Boxplots showing hydrochemical concentrations of remaining ions at the outflow of the stream of ICW for 2014 (grey), 2015 (orange), and 2016 (blue). Concentrations for  $\text{PO}_4$  were only measured in 2015 and 2016 and are all below the detection limit, as well as values for  $P$  throughout all years. Note that values below the detection limit were set to the value of the detection limit.

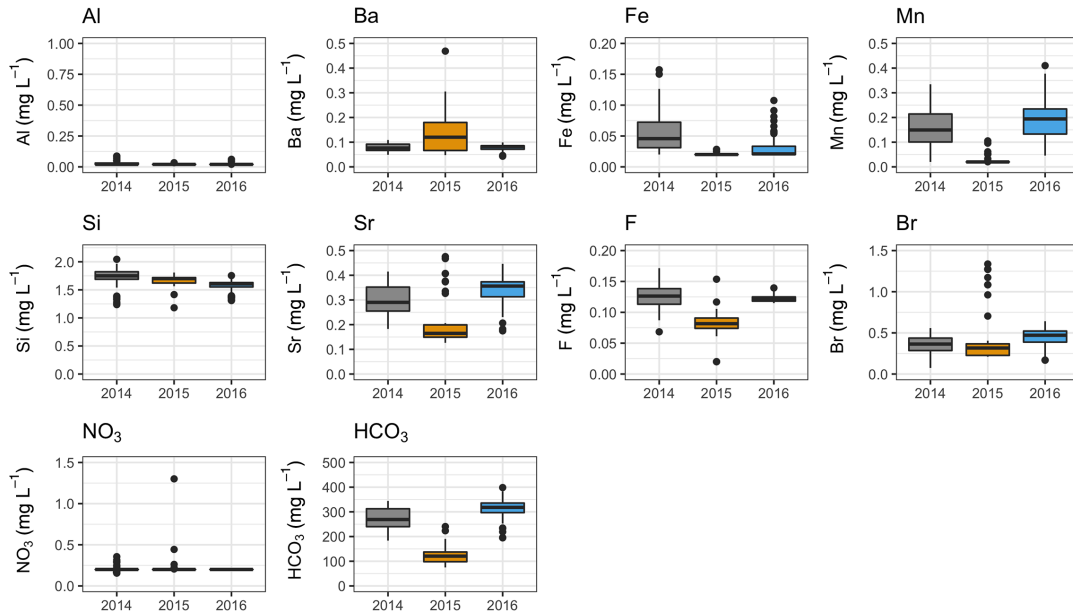


**Fig. A5.** Rainfall events 2014-1, 2015-1, 2015-2, 2015-3 showing rainfall and hydrograph response (top plot), discharge–TDS hysteresis, discharge–DOC hysteresis, and discharge–SSC hysteresis (below). The hysteresis line follows every time step from the beginning (green dot) to the end (red dot) of each rainfall event.

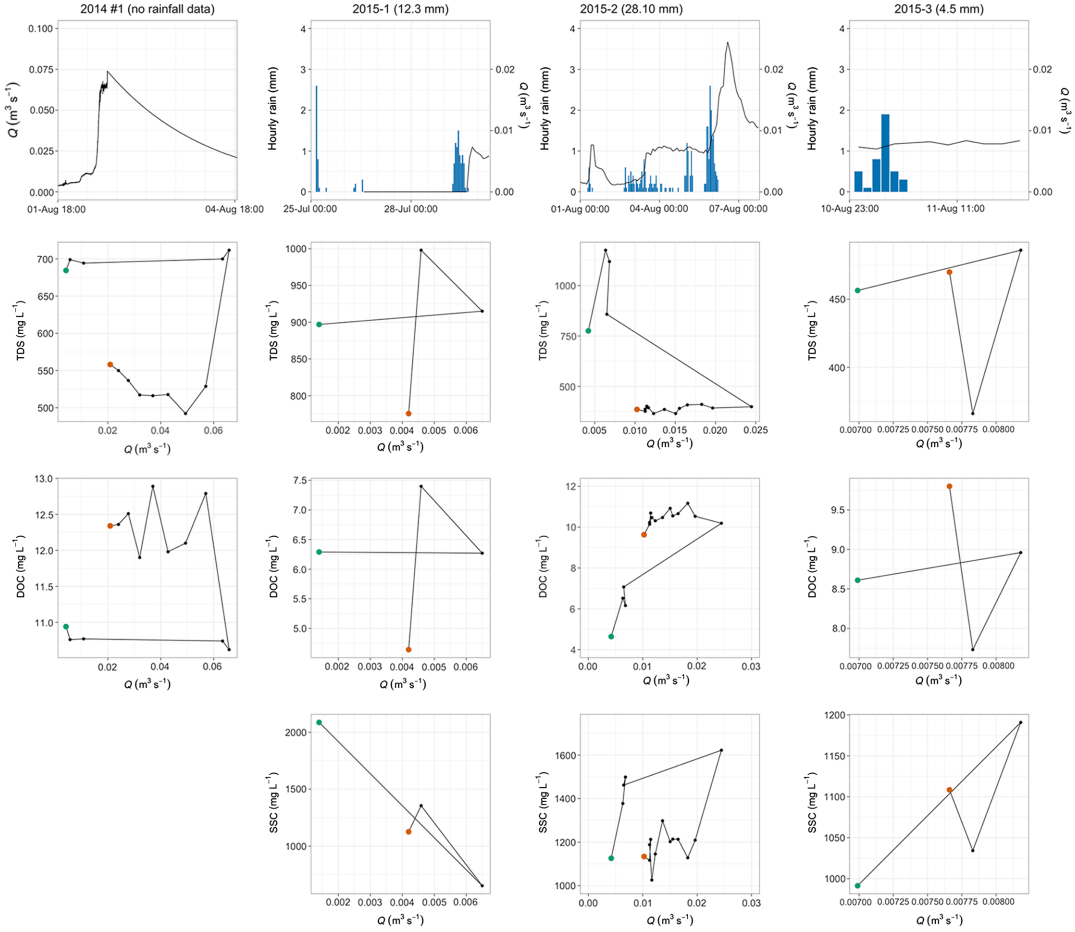


**Fig. A6.** Rainfall events 2016-1, 2016-2, 2016-3 showing rainfall and hydrograph response (top plot), discharge–TDS hysteresis, discharge–DOC hysteresis, and discharge–SSC hysteresis (below). The hysteresis line follows every time step from the beginning (green dot) to the end (red dot) of each rainfall event (continuation).

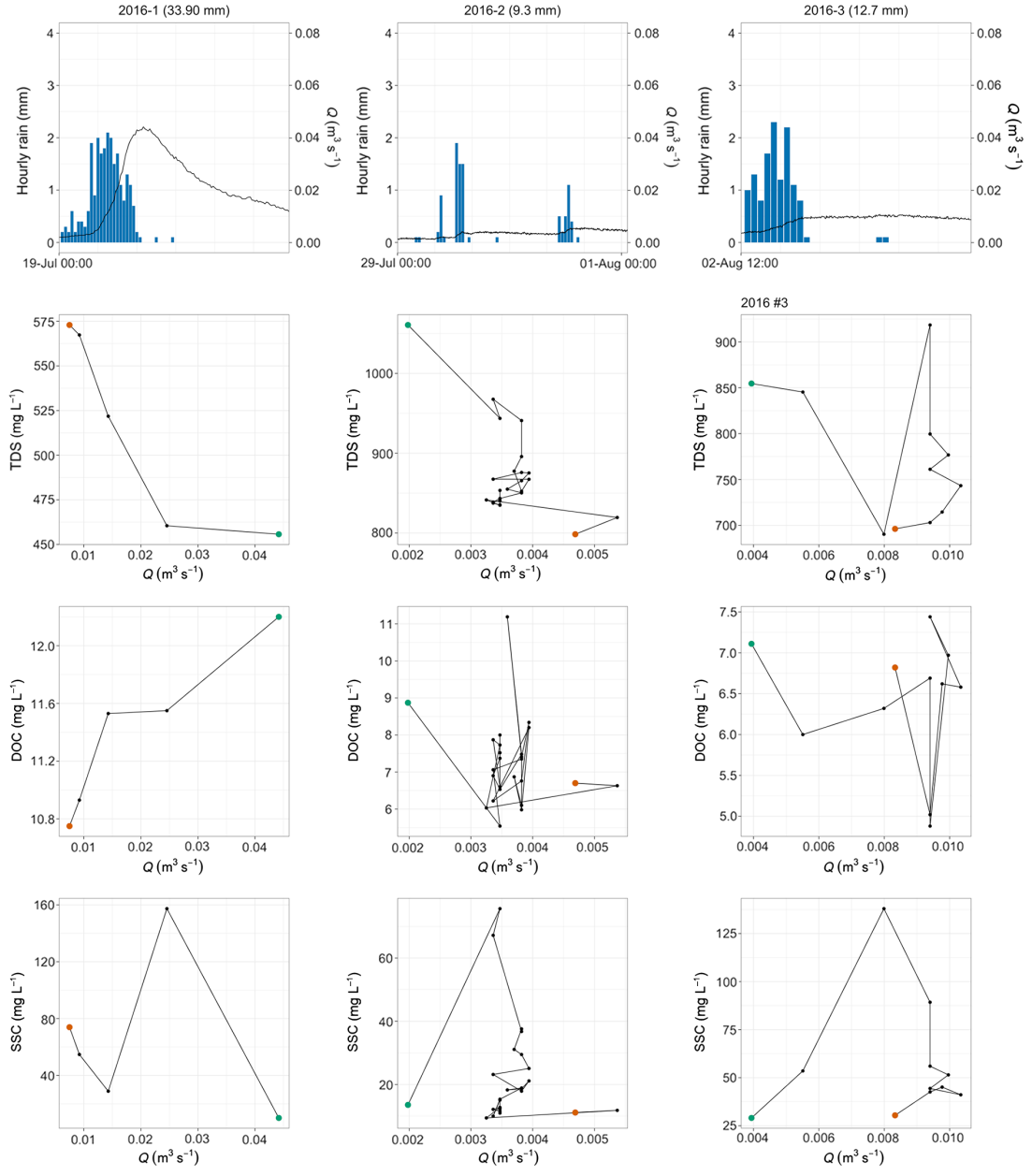


**Table A1.** Comparisons of means between the seasons for all measured parameters.

|                  | 2014 vs. 2015                   | 2015 vs. 2016                   | 2014 vs. 2016                   |
|------------------|---------------------------------|---------------------------------|---------------------------------|
| Al               | <b><math>p &lt; 0.05</math></b> | $p > 0.05$                      | $p < 0.05$                      |
| Ba               | <b><math>p &lt; 0.05</math></b> | <b><math>p &lt; 0.05</math></b> | $p > 0.05$                      |
| Ca               | <b><math>p &lt; 0.05</math></b> | <b><math>p &lt; 0.05</math></b> | <b><math>p &lt; 0.05</math></b> |
| Fe               | <b><math>p &lt; 0.05</math></b> | <b><math>p &lt; 0.05</math></b> | <b><math>p &lt; 0.05</math></b> |
| K                | <b><math>p &lt; 0.05</math></b> | <b><math>p &lt; 0.05</math></b> | $p > 0.05$                      |
| Mg               | <b><math>p &lt; 0.05</math></b> | <b><math>p &lt; 0.05</math></b> | $p > 0.05$                      |
| Mn               | <b><math>p &lt; 0.05</math></b> | <b><math>p &lt; 0.05</math></b> | <b><math>p &lt; 0.05</math></b> |
| Na               | <b><math>p &lt; 0.05</math></b> | <b><math>p &lt; 0.05</math></b> | <b><math>p &lt; 0.05</math></b> |
| P                | NA                              | NA                              | NA                              |
| Si               | $p > 0.05$                      | <b><math>p &lt; 0.05</math></b> | <b><math>p &lt; 0.05</math></b> |
| Sr               | <b><math>p &lt; 0.05</math></b> | <b><math>p &lt; 0.05</math></b> | <b><math>p &lt; 0.05</math></b> |
| F                | <b><math>p &lt; 0.05</math></b> | <b><math>p &lt; 0.05</math></b> | $p > 0.05$                      |
| Cl               | <b><math>p &lt; 0.05</math></b> | <b><math>p &lt; 0.05</math></b> | <b><math>p &lt; 0.05</math></b> |
| SO <sub>4</sub>  | $p > 0.05$                      | <b><math>p &lt; 0.05</math></b> | <b><math>p &lt; 0.05</math></b> |
| Br               | $p > 0.05$                      | $p > 0.05$                      | <b><math>p &lt; 0.05</math></b> |
| NO <sub>3</sub>  | <b><math>p &lt; 0.05</math></b> | $p > 0.05$                      | <b><math>p &lt; 0.05</math></b> |
| PO <sub>4</sub>  | NA                              | NA                              | NA                              |
| HCO <sub>3</sub> | <b><math>p &lt; 0.05</math></b> | <b><math>p &lt; 0.05</math></b> | <b><math>p &lt; 0.05</math></b> |
| DOC              | <b><math>p &lt; 0.05</math></b> | <b><math>p &lt; 0.05</math></b> | <b><math>p &lt; 0.05</math></b> |
| TDN              | NA                              | <b><math>p &lt; 0.05</math></b> | NA                              |
| TDS              | <b><math>p &lt; 0.05</math></b> | <b><math>p &lt; 0.05</math></b> | <b><math>p &lt; 0.05</math></b> |
| SSC              | NA                              | <b><math>p &lt; 0.05</math></b> | NA                              |
| POC              | NA                              | NA                              | NA                              |

**Note:** The student's *t* test was applied for normally distributed data; the Wilcoxon rank sum test for not normally distributed data. A *p* value below 0.05 means that there is a significant difference in the mean (marked in bold). DOC, dissolved organic carbon; TDN, total dissolved nitrogen; SSC, suspended sediment concentration; POC, particulate organic carbon; and TDS, total dissolved solids; NA, not available.

**Table A2.** Summary of all measured variables in Ice Creek West between 2014 and 2016.

|  | 2014  |       |       |           |     |    | 2015   |       |        |           |     |    | 2016  |       |        |           |     |    |       |
|--|-------|-------|-------|-----------|-----|----|--------|-------|--------|-----------|-----|----|-------|-------|--------|-----------|-----|----|-------|
|  | Mean  | Min   | Max   | Std. dev. | BDL | n  | Mean   | Min   | Max    | Std. dev. | BDL | n  | Mean  | Min   | Max    | Std. dev. | BDL | n  | Rain  |
| July to August (°C)                    | 7.9   | -0.5  | 21.0  | 2.6       | NA  | NA | 7.7    | 0.3   | 21.7   | 3.4       | NA  | NA | 8.5   | 0.5   | 26.6   | 3.4       | NA  | NA | NA    |
| Q (m <sup>3</sup> s <sup>-1</sup> )    | 0.012 | 0.001 | 0.074 | 0.016     | NA  | NA | 0.007  | 0.001 | 0.024  | 0.004     | NA  | NA | 0.005 | 0.001 | 0.044  | 0.004     | NA  | NA | NA    |
| DOC (mg L <sup>-1</sup> )              | 11.1  | 9.7   | 12.9  | 0.8       | 0   | 60 | 8.8    | 1.0   | 11.2   | 2.1       | 1   | 36 | 8.0   | 4.9   | 12.2   | 1.8       | 0   | 66 | NA    |
| TDN (mg L <sup>-1</sup> )              | NA    | NA    | NA    | NA        | 0   | 60 | 0.5    | 0.5   | 0.9    | 0.1       | 7   | 36 | 0.5   | 0.5   | 0.7    | 0.1       | 39  | 66 | NA    |
| SSC (mg L <sup>-1</sup> )              | NA    | NA    | NA    | NA        | 0   | 60 | 1180.0 | 167.5 | 2087.1 | 280.1     | 0   | 36 | 28.5  | 5.7   | 157.3  | 28.2      | 0   | 65 | NA    |
| POC (mg L <sup>-1</sup> )              | NA    | NA    | NA    | NA        | 0   | 60 | NA     | NA    | NA     | NA        | NA  | NA | 0.7   | 0.2   | 2.7    | 0.6       | 0   | 36 | NA    |
| TDS (mg L <sup>-1</sup> )              | 738.3 | 492.2 | 957.0 | 134.1     | 0   | 60 | 552.9  | 364.6 | 1176.2 | 246.8     | 0   | 36 | 814.6 | 455.7 | 1060.7 | 121.4     | 0   | 66 | 83.3  |
| Al (µg L <sup>-1</sup> )               | 28.9  | 20.0  | 87.3  | 16.3      | 37  | 60 | 20.4   | 20.0  | 33.7   | 2.2       | 35  | 36 | 21.2  | 20.0  | 61.1   | 6.0       | 62  | 66 | <20   |
| Ba (µg L <sup>-1</sup> )               | 77.2  | 49.0  | 108.8 | 15.2      | 0   | 60 | 134.0  | 47.4  | 468.7  | 87.1      | 0   | 36 | 79.2  | 43.1  | 99.1   | 11.6      | 0   | 66 | <20   |
| Ca (mg L <sup>-1</sup> )               | 79.4  | 49.8  | 109.3 | 16.2      | 0   | 60 | 45.5   | 25.3  | 100.6  | 22.6      | 0   | 36 | 85.0  | 44.8  | 111.0  | 13.0      | 0   | 66 | 14.0  |
| Fe (µg L <sup>-1</sup> )               | 55.6  | 20.0  | 157.3 | 31.7      | 2   | 60 | 20.4   | 20.0  | 28.4   | 1.6       | 34  | 36 | 31.3  | 20.0  | 107.5  | 18.7      | 32  | 66 | <20   |
| K (mg L <sup>-1</sup> )                | 6.6   | 4.7   | 8.9   | 1.1       | 0   | 60 | 6.1    | 2.8   | 23.1   | 4.7       | 0   | 36 | 6.4   | 3.8   | 8.7    | 1.1       | 0   | 66 | 1.2   |
| Mg (mg L <sup>-1</sup> )               | 32.1  | 20.1  | 44.4  | 6.0       | 0   | 60 | 25.2   | 16.4  | 52.2   | 11.6      | 0   | 36 | 31.9  | 17.2  | 43.0   | 5.1       | 0   | 66 | 1.4   |
| Mn (µg L <sup>-1</sup> )               | 160.8 | 20.0  | 334.5 | 84.8      | 2   | 60 | 27.8   | 20.0  | 105.2  | 20.2      | 28  | 36 | 193.7 | 45.7  | 410.1  | 74.9      | 0   | 66 | 21.0  |
| Na (mg L <sup>-1</sup> )               | 108.0 | 71.0  | 146.7 | 20.1      | 0   | 60 | 96.7   | 59.8  | 215.8  | 45.3      | 0   | 36 | 119.3 | 65.5  | 159.6  | 20.1      | 0   | 66 | 6.1   |
| P (mg L <sup>-1</sup> )                | <0.1  | <0.1  | <0.1  | 0.0       | 60  | 60 | <0.1   | <0.1  | <0.1   | 0.0       | 36  | 36 | <0.1  | <0.1  | <0.1   | 0.0       | 66  | 66 | <0.1  |
| Si (mg L <sup>-1</sup> )               | 1.7   | 1.2   | 2.0   | 0.2       | 0   | 60 | 1.7    | 1.2   | 1.8    | 0.1       | 0   | 36 | 1.6   | 1.3   | 1.8    | 0.1       | 0   | 66 | <0.1  |
| Sr (µg L <sup>-1</sup> )               | 296.3 | 182.6 | 414.9 | 61.1      | 0   | 60 | 211.9  | 126.4 | 475.6  | 102.8     | 0   | 36 | 340.8 | 174.9 | 446.4  | 54.2      | 0   | 66 | 25.0  |
| F (mg L <sup>-1</sup> )                | 0.1   | 0.1   | 0.2   | 0.0       | 0   | 60 | 0.1    | 0.0   | 0.2    | 0.0       | 2   | 36 | 0.1   | 0.1   | 0.1    | 0.0       | 0   | 66 | <0.05 |
| Cl (mg L <sup>-1</sup> )               | 195.8 | 124.8 | 265.3 | 41.5      | 0   | 60 | 201.3  | 120.2 | 458.4  | 103.4     | 0   | 36 | 210.1 | 102.9 | 272.8  | 37.8      | 0   | 66 | 9.9   |
| SO <sub>4</sub> (mg L <sup>-1</sup> )  | 41.1  | 28.7  | 54.9  | 7.5       | 0   | 60 | 50.6   | 27.5  | 126.6  | 32.4      | 0   | 36 | 44.7  | 23.8  | 65.5   | 8.5       | 0   | 66 | 5.3   |
| Br (mg L <sup>-1</sup> )               | 0.4   | 0.1   | 0.6   | 0.1       | 0   | 60 | 0.5    | 0.2   | 1.3    | 0.4       | 0   | 36 | 0.4   | 0.2   | 0.6    | 0.1       | 0   | 66 | 0.1   |
| NO <sub>3</sub> (mg L <sup>-1</sup> )  | 0.2   | 0.2   | 0.4   | 0.0       | 36  | 60 | 0.2    | 0.2   | 1.3    | 0.2       | 31  | 36 | <0.2  | <0.2  | <0.2   | 0.0       | 66  | 66 | 3.9   |
| PO <sub>4</sub> (mg L <sup>-1</sup> )  | NA    | NA    | NA    | NA        | 60  | 60 | <0.1   | <0.1  | <0.1   | 0.0       | 36  | 36 | <0.1  | <0.1  | <0.1   | 0.0       | 66  | 66 | <0.1  |
| HCO <sub>3</sub> (mg L <sup>-1</sup> ) | 272.5 | 183.5 | 344.1 | 45.7      | 0   | 60 | 125.0  | 74.9  | 240.6  | 37.1      | 0   | 36 | 314.3 | 194.8 | 398.4  | 40.0      | 0   | 66 | 45.3  |

**Note:** Mean, minimum, maximum, and standard deviation number of samples below detection limit (BDL) and total number of samples (n) are reported. DOC, dissolved organic carbon; TDN, total dissolved nitrogen; SSC, suspended sediment concentration; POC, particulate organic carbon; and TDS, total dissolved solids; NA, not available.

## Appendix B

Time lapse video of the river channel during the nival period: 25 Apr. to 31 May 2016 (see [supplementary material](#)).<sup>1</sup>

### Reference

Environment and Climate Change Canada. 2018. Historical Data. Environment and Climate Change Canada. [Online]. Available from [http://climate.weather.gc.ca/historical\\_data/search\\_historic\\_data\\_e.html](http://climate.weather.gc.ca/historical_data/search_historic_data_e.html) [05 Apr. 2018].